

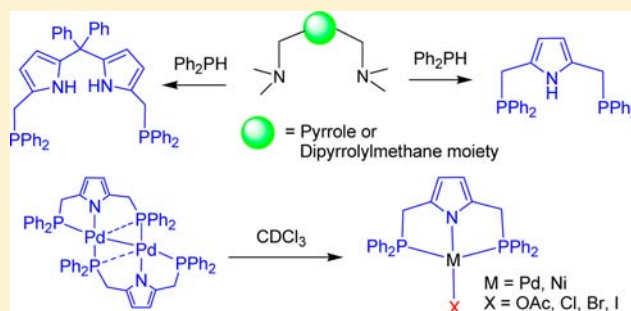
Pyrrole-Based New Diphosphines: Pd and Ni Complexes Bearing the PNP Pincer Ligand

Shanish Kumar, Ganesan Mani,* Sukanta Mondal, and Pratim Kumar Chattaraj

Department of Chemistry, Indian Institute of Technology, Kharagpur, India 721 302

Supporting Information

ABSTRACT: A new class of diphosphine PNP pincer ligand, 2,5-bis(diphenylphosphinomethyl)pyrrole **2**, was synthesized by the reaction between Ph_2PH and 2,5-bis(dimethylaminomethyl)pyrrole in 90% yield. The analogous reaction of Ph_2PH with 1,9-bis(dimethylaminomethyl)-diphenyldipyrrolylmethane readily afforded a PNNP type diphosphine ligand, 1,9-bis(diphenylphosphinomethyl)-diphenyldipyrrolylmethane **5** in 92% yield. These phosphine compounds were oxidized with H_2O_2 and S_8 to give the corresponding phosphoryl and thiophosphoryl compounds **6–9** in very good yields. The reaction of the PNP pincer ligand **2** with $[\text{PdCl}_2(\text{PhCN})_2]$ in the presence of Et_3N afforded the mononuclear Pd(II) complex, $[\text{PdCl}\{\text{C}_4\text{H}_2\text{N}-2,5-(\text{CH}_2\text{PPh}_2)_2-\kappa^3\text{PNP}\}]$ **10** in 87% yield. Conversely, treatment of **2** with $[\text{PdCl}_2(\text{PhCN})_2]$ in the absence of Et_3N gave the dinuclear Pd(II) complex $[\text{Pd}_2\text{Cl}_4\{\mu-\text{C}_4\text{H}_2\text{N}-2,5-(\text{CH}_2\text{PPh}_2)_2-\kappa^2\text{PP}\}_2]$, the structure which is proposed based on the spectroscopic data. When **2** was treated with Pd(0) precursor $[\text{Pd}_2(\text{dba})_3]\cdot\text{CHCl}_3$ the dinuclear Pd(I) complex $[\text{Pd}_2\{\mu-\text{C}_4\text{H}_2\text{N}-2,5-(\text{CH}_2\text{PPh}_2)_2-\kappa^2\text{PN},\kappa^1\text{P}\}_2]$, **12**, was obtained in 23% yield. The formation of complex **12** is solvent dependent, which transforms into complex **10** in CDCl_3 as studied by variable temperature ^1H and ^{31}P NMR methods. Treatment of **2** with $[\text{Ni}(\text{OAc})_2]\cdot 4\text{H}_2\text{O}$ gave the mononuclear Ni(II) pincer complex $[\text{Ni}(\text{OAc})\{\text{C}_4\text{H}_2\text{N}-2,5-(\text{CH}_2\text{PPh}_2)_2-\kappa^3\text{PNP}\}]$, **13**, which upon treatment with an excess of LiCl or LiBr or KI afforded the respective halide ion substituted Ni(II) complexes, $[\text{NiX}\{\text{C}_4\text{H}_2\text{N}-2,5-(\text{CH}_2\text{PPh}_2)_2-\kappa^3\text{PNP}\}]$ ($\text{X} = \text{Cl}, \text{Br}, \text{and I}$), **14–16**, in very good yields. The structures of **5**, 2,5-bis(diphenylphosphorylmethyl)pyrrole **6**, **10**, **12**, and **14–16** were determined by the single crystal X-ray diffraction method. In the structure of **12**, two short contacts between the diagonally positioned Pd and P atoms are observed. To understand these weak interactions, density functional theory (DFT) calculations were done and an interaction MO diagram is presented.



INTRODUCTION

Metal complexes containing a pincer framework ligand continue to attract attention because of their ability in providing the required combination of stability and reactivity with metal complexes.¹ The framework of a pincer ligand can be modified in terms of both steric and electronic factors to modulate the property of a metal center, which has led to development of several types of pincer ligands.² Pincer ligands coordinate in L_3 , L_2X , LX_2 , and X_3 fashions to metal centers.³ Such coordination modes often maintain a rigid planarity with metal centers.⁴ Pincer complexes have been shown to be very active catalysts for various organic transformation reactions such as alkane dehydrogenation,⁵ dehydrogenation of alcohols,⁶ activation of small molecules,⁷ Suzuki,⁸ Heck,⁹ Kumada¹⁰ and olefin polymerization reactions¹¹ among others¹² and act as platforms to understand mechanistic details of very important reactions such as activation of C–C,¹³ C–N,¹⁴ C–O,¹⁵ and C–H¹⁶ bond. Pincer ligands are classified as EZE' where E and E' are usually neutral donor atoms and Z is a central monoanionic or neutral donor atom. Among the known types of pincer ligands, pincer ligands containing a P donor such as PCP,¹⁷

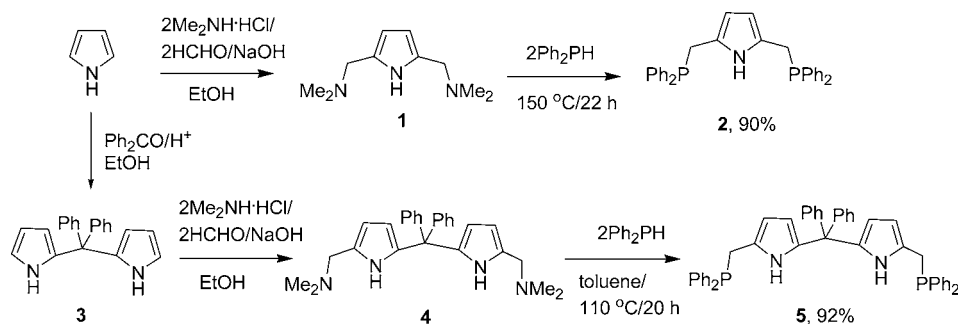
PCN,¹⁸ PNN,¹⁹ and PNP²⁰ have attracted great attention right from the first pincer ligand (PCP) reported in 1976.²¹ Typically, several of these PCP or other pincer ligands have a six-membered aromatic ring which supplies the central atom. In contrast to this, only a few pincer ligands whose central atom comes from a pyrrole ring have been reported.²² Recently, we reported the synthesis of a new NNN pincer ligand containing a pyrrole unit which supplies the central atom and its Pd and Ni complexes.²³

As a continuation of our interests to develop pyrrole-based pincer ligands, we set to synthesize new pyrrole-based pincer ligands containing P donors for exploring metal complexes and their catalytic applications. Herein, we report a simple synthetic method for the preparation of a new class of pyrrole-based PNP and the dipyrrolylmethane-based PNNP type diphosphine ligands, and their oxidized products. In addition, we report the synthesis and structural characterization of Pd(II), Pd(I), and Ni(II) complexes containing the PNP pincer ligand together

Received: September 9, 2012

Published: November 8, 2012

Scheme 1. Synthesis of the Pyrrole-Based PNP Pincer (2) and PNNP Type (5) Diphosphines



with density functional theory (DFT) calculations on the Pd(I) dimer. However, after our work was submitted to this journal, a paper describing the synthesis of the compounds **2**, **14**, and **16** was submitted to Dalton Transactions and published online.²⁴

RESULTS AND DISCUSSION

Synthesis and Characterization of P(III) and P(V) Ligands. The reaction between a double Mannich base of pyrrole, 2,5-bis(dimethylaminomethyl)pyrrole **1**, and 2 equiv of Ph₂PH at elevated temperature in the absence of any solvent cleanly afforded a new PNP pincer diphosphine ligand, 2,5-bis(diphenylphosphinomethyl)pyrrole **2**, in 90% yield. The analogous reaction of Ph₂PH with 1,9-bis(dimethylaminomethyl)dipyrrolylmethane under reflux condition readily afforded a new PNNP type diphosphine ligand, 1,9-bis(diphenylphosphinomethyl)dipyrrolylmethane **5**, in 92% yield (Scheme 1). These compounds were formed by the nucleophilic substitution of dimethylamide (NMe₂⁻) by diphenylphosphide (Ph₂P⁻) group and were obtained in a pure form just by removing volatiles of the reaction mixture. Earlier we reported a pyrrole-based NNN pincer ligand, 2,5-bis(3,5-dimethylpyrazolylmethyl)pyrrole, by this synthetic strategy which is the reaction between 2,5-bis(dimethylaminomethyl)pyrrole and 3,5-dimethylpyrazole.²³

The diphosphine compounds **2** and **5** are solid at room temperature and soluble in common organic solvents. The ¹H NMR spectra of **2** and **5** in CDCl₃ feature broad singlets at δ = 7.67 and 7.53 ppm for their NH protons, respectively. The ³¹P{¹H}NMR spectra show a singlet at δ -16.3 ppm for **2** and at δ -15.5 ppm for **5**, suggesting that both phosphorus atoms of **2** or **5** are in equivalent environments. In addition, the structure of **5** was further confirmed by the X-ray diffraction method (Figure 1 and Table 1). The X-ray structure revealed that the two pyrrolic NH groups are oriented in opposite directions with the two phosphorus centers pyramidalized in opposite directions, which thus minimizes steric crowding.

It is noteworthy that these new diphosphine ligands were synthesized without using an air-sensitive reactant Ph₂PLi which upon reaction with **1** or **4** or their quaternary ammonium salts could lead to the formation of **2** or **5**, respectively. For example, the reaction between **1** or its quaternary ammonium salt and 2 equiv of Ph₂PLi in tetrahydrofuran (THF) gave a mixture of products. The ³¹P NMR spectrum of this reaction mixture in CDCl₃ showed a singlet at -16.3 ppm, which is the signal of **2**, together with the resonance of Ph₂PH and other unidentified products. In view of these, the direct reaction of Ph₂PH with the Mannich bases is a simple and clean method, and involves two and three steps starting from pyrrole using

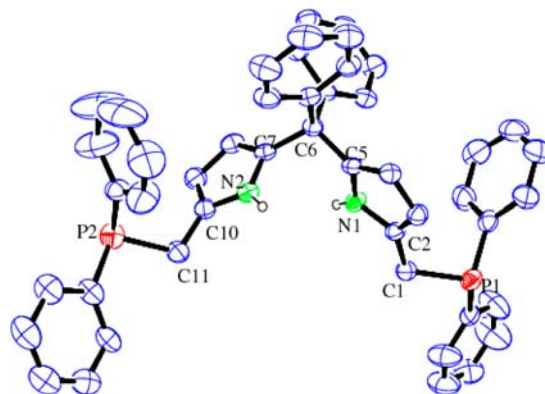


Figure 1. ORTEP diagram of 1,9-bis(diphenylphosphinomethyl)dipyrrolylmethane, **5** (30% thermal ellipsoids). All hydrogen atoms except the pyrrolic NH are omitted for clarity. Selected bond lengths (Å) and angles (deg): P1–C1 1.846(6), C1–C2 1.501(7), C2–N1 1.368(7), C5–C6 1.521(8), P1–C1–C2 112.6(4), C5–C6–C7 111.6(5).

which the diphosphine ligands **2** and **5** can be synthesized in multigram scales, respectively.

The trivalent phosphorus centers in **2** and **5** were converted to their pentavalent phosphorus centers by the oxidation reactions shown in Scheme 2. Thus, the treatment of **2** or **5** with an aqueous H₂O₂ in toluene gave the phosphoryl compound **6** or **8**, respectively. The analogous reaction between **2** or **5** with the elemental S₈ in toluene yielded the thiophosphoryl compound **7** or **9** in very good yields, respectively. These compounds were primarily characterized by spectroscopic methods. One of the interesting features of their ¹H NMR spectra, in contrast to those shown by the trivalent phosphorus compounds **2** and **5**, is the signal due to the methylene protons, which appears as a doublet, owing to coupling with the phosphorus atoms, in the deshielded region as compared to the resonances of the methylene protons in **2** and **5**. Similarly, the NH resonances appear as a broad singlet in the deshielded region. The ³¹P{¹H} spectrum of each compound **6–9** in CDCl₃ gives a singlet in the deshielded region as compared to the chemical shift value at which the parent compound resonates. This indicates that P(III) centers are changed to P(V) centers which are in equivalent environments. Further, the ³¹P chemical shift differences (Δδ = 55.1 ppm for **7** and Δδ = 54.8 ppm for **9**) observed for the thiophosphoryl compounds are larger than those (Δδ = 47.8 ppm for **6** and 47.1 ppm for **8**) observed for the phosphoryl compounds; this is in line with the values of Δδ reported for Ph₃PO and Ph₃PS.²⁵

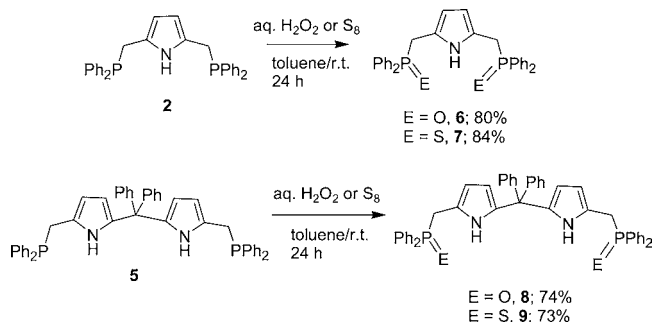
Table 1. Crystallographic Data for Compounds 5, 6, 10, 12, and 14–16

	5	(6·2H ₂ O) ₂	10	12·0.5(C ₆ H ₆)
empirical formula	C ₄₇ H ₄₀ N ₂ P ₂	C ₆₀ H ₆₂ N ₂ O ₈ P ₄	C ₃₀ H ₂₆ NP ₂ ClPd	C ₆₃ H ₅₅ N ₂ P ₄ Pd ₂
formula weight	694.75	1063.00	604.31	1176.77
wavelength (Å)	0.71073	0.71073	0.71073	0.71073
temperature (K)	295(2)	295(2)	295(2)	295(2)
crystal system	monoclinic	triclinic	monoclinic	triclinic
color and shape	colorless, needle	colorless, prism	yellow, prism	orange, prism
space group	C2/c	P $\bar{1}$	P2(1)/c	P $\bar{1}$
a/Å	28.352(3)	9.873(3)	14.438(3)	13.7600(9)
b/Å	10.4594(11)	13.325(4)	16.355(3)	14.2819(9)
c/Å	26.729(3)	22.878(7)	11.664(2)	16.0506(11)
α /deg	90.0	91.246(10)	90.0	66.630(2)
β /deg	103.113(3)	99.788(11)	107.914(7)	69.334(2)
γ /deg	90.0	109.750(9)	90.0	85.481(2)
volume (Å ³)	7719.9(13)	2781.3(16)	2620.9(9)	2702.3(3)
Z	8	2	4	2
D _{calcd} g cm ⁻³	1.169	1.269	1.531	1.446
μ /mm ⁻¹	0.148	0.192	0.952	0.826
F(000)	2928	1120	1224	1198
crystal size/mm	0.44 × 0.17 × 0.08	0.50 × 0.25 × 0.13	0.31 × 0.16 × 0.05	0.27 × 0.19 × 0.14
θ range (deg)	1.47 to 20.82	0.91 to 25.19	1.48 to 25.00	1.48 to 26.28
limiting indices	-26 ≤ h ≤ 28, -10 ≤ k ≤ 10, -26 ≤ l ≤ 26	-11 ≤ h ≤ 11 -15 ≤ k ≤ 15 -27 ≤ l ≤ 27	-17 ≤ h ≤ 17 -19 ≤ k ≤ 19 -13 ≤ l ≤ 13	-17 ≤ h ≤ 16, -17 ≤ k ≤ 17, -19 ≤ l ≤ 19
total/unique no. of refls.	30151/4027	33621/9853	30979/4603	34841/10698
R _{int}	0.1313	0.0892	0.1523	0.0637
data/restr./ params.	4027/0/468	9853/4/691	4603/0/316	10698/0/631
GOF (F ²)	0.998	1.000	1.002	1.023
RI, wR2	0.0632, 0.1456	0.0608, 0.1408	0.0480, 0.0847	0.0474, 0.0920
R indices (all data) RI, wR2	0.1284, 0.1809	0.1528, 0.1845	0.1070, 0.1044	0.1007, 0.1133
largest different peak and hole (e Å ⁻³)	1.004 and -0.286	0.413 and -0.280	0.501 and -0.617	0.581 and -0.376
	14	15	16	
empirical formula	C ₃₀ H ₂₆ ClNNiP ₂	C ₃₀ H ₂₆ BrNNiP ₂	C ₃₀ H ₂₆ INNiP ₂	
formula weight	556.62	601.08	648.07	
wavelength (Å)	0.71073	0.71073	0.71073	
temperature (K)	295(2)	295(2)	295(2)	
crystal system	monoclinic	monoclinic	monoclinic	
color and shape	orange, plate	brown, prism	purple, plate	
space group	P2(1)/c	P2(1)/c	P2(1)/c	
a/Å	14.423(3)	14.407(2)	14.436(5)	
b/Å	16.338(3)	16.410(3)	16.639(5)	
c/Å	11.552(2)	11.576(18)	11.587(5)	
α /deg	90.0	90.0	90.0	
β /deg	107.125(6)	107.282(5)	107.151(5)	
γ /deg	90.0	90.0	90.0	
volume (Å ³)	2601.3(9)	2609.2(7)	2659.4(17)	
Z	4	4	4	
D _{calcd} g cm ⁻³	1.421	1.530	1.619	
μ /mm ⁻¹	0.992	2.418	2.031	
F(000)	1152	1224	1296	
crystal size/mm	0.58 × 0.29 × 0.08	0.20 × 0.19 × 0.17	0.41 × 0.22 × 0.03	
θ range (degree)	1.93 to 24.99	1.48 to 24.99	1.187 to 25.00	
limiting indices	-15 ≤ h ≤ 17, -19 ≤ k ≤ 19, -13 ≤ l ≤ 13	-16 ≤ h ≤ 17, -19 ≤ k ≤ 19, -13 ≤ l ≤ 13	-17 ≤ h ≤ 15, 19 ≤ k ≤ 19, -13 ≤ l ≤ 13	
total/unique no. of refls.	30783/4572	30557/4586	30643/4670	
R _{int}	0.0642	0.1084	0.0521	
data/restr./ params.	4572/0/316	4586/0/316	4670/0/316	
GOF (F ²)	1.036	1.027	1.075	
RI, wR2	0.0361, 0.0839	0.0410, 0.0721	0.0304, 0.0641	
R indices (all data) RI, wR2	0.0620, 0.0955	0.0947, 0.0913	0.0491, 0.0805	

Table 1. continued

	14	15	16
largest different peak and hole ($e \text{ \AA}^{-3}$)	0.398 and -0.229	0.371 and -0.412	0.404 and -0.549

Scheme 2. Synthesis of the Phosphoryl and Thiophosphoryl Compounds 6–9



The structure of **6** was determined by a X-ray diffraction study (Figure 2 and Table 1). Compound **6** crystallizes in the

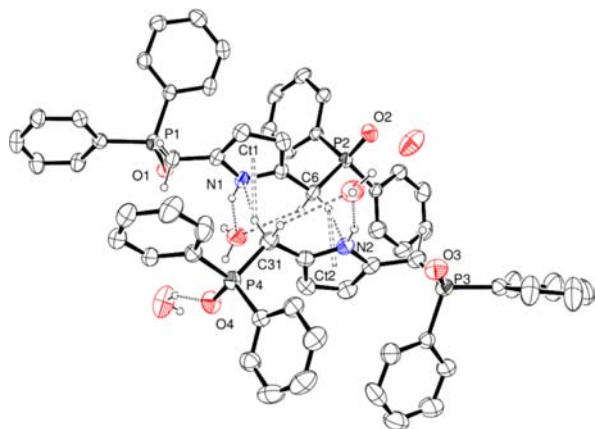
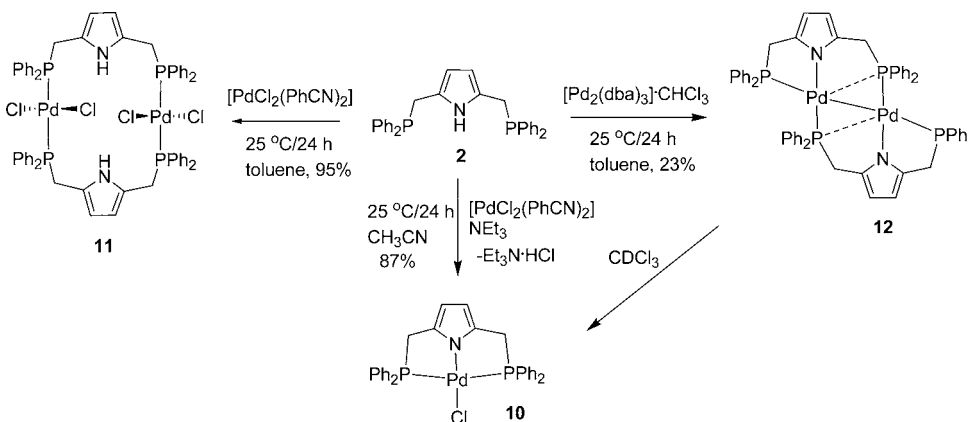


Figure 2. ORTEP diagram of $(6 \cdot 2\text{H}_2\text{O})_2$ with 30% probability ellipsoids. Most H atoms are omitted for clarity. Selected bond lengths (Å) and angles (deg): O1–P1 1.493(3), O3–P3 1.483(3), O4–P4 1.486(3), C1–P1 1.814(4), C25–P1 1.802(4), C2–N1 1.375(5), C2–C1–P1 115.2(3), O1–P1–C25 112.11(19), C25–P1–C1 105.26(19), C19–P1–C25 107.92(19), N1–C2–C1 122.4(4), C6···N2 3.574, H6b···N2 2.674, C6–H6b···N2 154.60; C31···N1 3.684, H31a···N1 2.789, C31–H31a···N1 153.82.

$P\bar{1}$ space group with two molecules in the asymmetric unit along with four water molecules. As shown in Figure 2, two molecules of **6** are held together primarily via methylene $\text{CH} \cdots \pi$ interactions involving π electrons of the pyrrole ring. The pyrrolic NH groups are oriented in opposite directions and hydrogen bonded to the water molecules. One of the methylene group hydrogen atoms of each molecule is oriented more toward the center of the pyrrole ring of the adjacent molecule, resulting in two intermolecular $\text{CH} \cdots \pi$ (pyrrole) interactions. The observed bond lengths and angles support this $\text{CH} \cdots \pi$ interaction: C6···Ct2 3.381 Å, H6b··· Ct2 2.501 Å, C6–H6b···Ct2 150.96° and C31···Ct1 3.542 Å, H31a···Ct1 2.654 Å, C31–H31a···Ct1 152.38° (Ct = the centroid of a pyrrole ring), which are similar to the reported $\text{CH} \cdots \pi$ interaction with pyrrole ring.²⁶ These interactions are further facilitated by the orientation of the two phosphoryl groups (Ph_2PO) of each molecule; the “ Ph_2PO ” groups are bent away from the plane formed by the pyrrole ring and the two methylene carbons. The P–O and the P–C (methylene) bond distances are similar to those reported for other phosphine oxide compounds.²⁷

Synthesis and Characterization of Pd Complexes.

Having synthesized the new PNP and PNNP type diphosphine ligands in high yields, we set out to explore the coordination chemistry of the PNP pincer ligand by reacting with Pd(II), Pd(0), and Ni(II) precursors. As shown in Scheme 3, the reaction between an equimolar quantity of **2** and $[\text{PdCl}_2(\text{PhCN})_2]$ in the presence of NEt_3 afforded the mononuclear Pd(II) complex **10** in 87% yield after the workup procedure. The role of NEt_3 in this reaction is to facilitate the removal of HCl. This is in contrast to the reported reduction reactions giving Pd(I) complexes from Pd(II) precursors in the presence of NEt_3 .²⁸ Complex **10** was characterized by both spectroscopic and X-ray diffraction methods. The ^1H NMR spectrum of **10** in CDCl_3 shows a virtual triplet for the methylene protons, which is the characteristic of the $\text{mer-}\kappa^3\text{-PNP}$ coordination mode²⁹ and does not show a NH resonance. The absence of NH proton is further supported by the IR spectrum which does not show NH stretching frequency. Besides, the $^{31}\text{P}\{^1\text{H}\}$ NMR spectrum of **10** in CDCl_3 shows a singlet at $\delta = 33.8$ ppm, a downfield shift of 50.1 ppm

Scheme 3. Synthesis of the Mononuclear and Dinuclear Pd Complexes, 10–12, Bearing the PNP Pincer Ligand **2**

compared to that of the free ligand (^{31}P : $\delta = -16.3$ ppm), indicating that both the phosphorus centers of the ligand are having equivalent environments. These data indicate the presence of a monoanionic tridentate (*mer*- κ^3 -PNP) coordination mode of the pincer ligand in the structure of complex **10**.

The structure of **10** was confirmed by the X-ray diffraction method. The ORTEP diagram of the structure and the selected bond lengths and angles are given in Figure 3 and Table 2,

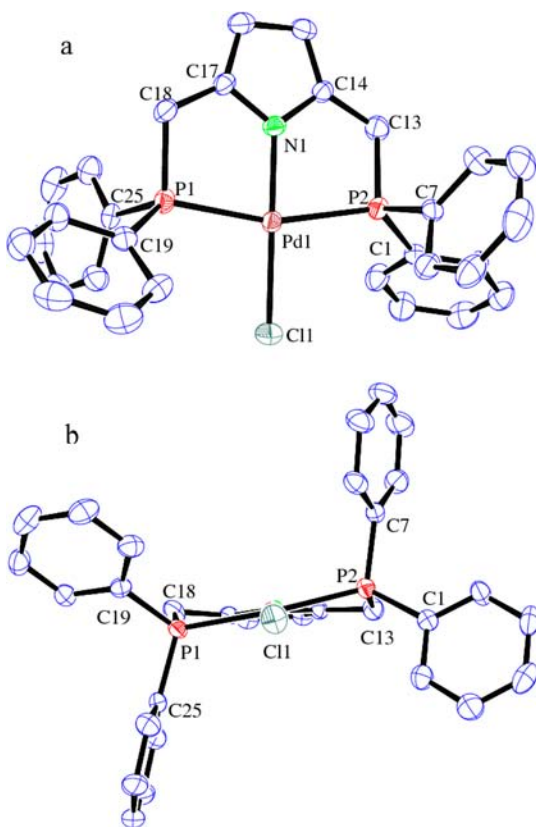


Figure 3. ORTEP diagram of the palladium complex **10** (30% thermal ellipsoids): (a) top view, and (b) side view, showing the twisted arrangement of the pincer ligand. All hydrogen atoms are omitted for clarity.

respectively. As shown in Figure 3, the ligand is slightly twisted and coordinated, and the structure possesses a C_2 axis passing through Pd–N bond. The two methylene carbon atoms are located above and below the plane defined by the four ligating atoms around the Pd center. This twisted conformation of the pincer ligand with the dihedral angle of P1–Pd1–N1–C17 = 2.29° and P2–Pd1–N1–C14 = 15.27° is similar to an

analogous Pd(II) pyridine-based pincer complex containing two fused five-membered rings.³⁰ The geometry around the Pd center is a distorted square planar with the Cl1–Pd1–P1 and Cl1–Pd1–P2 angles of 99.33° and 98.23° , respectively, which are larger than the other two angles (P1–Pd1–N1 = 81.53° and P2–Pd1–N1 = 81.07°). This angle difference is commonly observed for this type of complexes because of the steric factor with which the pincer ligand adopts a *mer*- κ^3 -PNP coordination mode. In addition, while the Pd–P bond distances (2.3074(16) Å and 2.2987(17) Å) and the Pd–Cl bond distance (2.3136(16) Å) are in the range reported for analogous mononuclear Pd complexes bearing a PNP pincer ligand,^{20f,30,31} the Pd–Cl bond distance is shorter than those (2.333 Å,^{17d} 2.395 Å³² and 2.397 Å³³) reported for analogous Pd complexes [(PCP)PdCl] bearing a PCP pincer ligand. This can be because of a weak trans influence of the pyrrolic nitrogen atom compared with that of the carbon atom in PCP pincer ligands.

On the contrary, the reaction of **2** with $[\text{PdCl}_2(\text{PhCN})_2]$ in the absence of a base afforded complex **11** in 95% yield (Scheme 3). The structure of **11** is proposed based on the spectroscopic and elemental analysis data. The ^1H NMR spectrum of complex **11** shows a broad singlet at $\delta = 9.86$ ppm for the pyrrolic NH protons. The presence of NH groups is further confirmed by the NH stretching frequency at 3344 cm^{-1} in the IR spectrum. The $^{31}\text{P}\{^1\text{H}\}$ NMR spectrum of **11** in CDCl_3 shows a singlet at $\delta = 14.3$ ppm, which is a downfield shift of 30.6 ppm compared to that of the free ligand and is in the upfield region as compared to complex **10** ($\delta = 33.8$ ppm) suggesting that the coordination fashion of the pincer ligand **2** can be different here. Further, the high resolution mass spectrometry electrospray ionization (HRMS, +ESI) spectrum of **11** shows peaks m/z at 1173.9480 (calcd 1173.0996) and at 1177.9426 (calcd 1177.0944) corresponding to the $[\text{M}-3\text{Cl}]^{3+}$ and the $[\text{M}-4\text{Cl}+\text{K}]^{5+}$ ions, respectively. Furthermore, the X-ray structure of an analogous dinuclear Pd(II) complex bearing the pincer ligand, 2,5-bis(3,5-dimethylpyrazolylmethyl)pyrrole, has been reported by us.²³ These data support the structure proposed for **11** in Scheme 3.

The reaction between 2 equiv of **2** and a Pd(0) precursor, $[\text{Pd}_2(\text{dba})_3]\cdot\text{CHCl}_3$, in toluene afforded a dinuclear Pd(I) complex **12** in 23% crystalline yield.³⁴ The ^1H NMR spectrum of **12** in CDCl_3 shows two ABX (A = H_A and B = H_B , X = P) spin patterns for the PCH₂ groups: one in the five-membered chelate ring and the other in the bridging six-membered ring, indicating the presence of two different phosphorus centers in the structure. However, the ^{31}P NMR spectrum which was recorded immediately after dissolving crystals of **12** in CDCl_3 or $\text{DMSO}-d_6$ does not show two doublets instead two singlets at $\delta = 17.6$ and 20.5 ppm are observed. Nonetheless, this

Table 2. Comparison of Bond Lengths (Å) and Angles (deg) for the Mononuclear Pd(II) and Ni(II) Complexes

complex	M–N	M–X	M–P1	M–P2		
[PNP]PdCl, 10	1.981(4)	2.3136(16)	2.3074(16)	2.2987(17)		
[PNP]NiCl, 14	1.855(2)	2.1699(9)	2.1990(9)	2.2063(9)		
[PNP]NiBr, 15	1.856(3)	2.3036(7)	2.2085(13)	2.1988(13)		
[PNP]NiI, 16	1.859(3)	2.4844(7)	2.1974(14)	2.2088(13)		
complex	N–M–P1	N–M–P2	P1–M–P2	P1–M–X	P2–M–X	N–M–X
[PNP]PdCl, 10	81.53(14)	81.07(14)	162.28(6)	99.33(6)	98.23(6)	176.82(14)
[PNP]NiCl, 14	82.94(7)	83.95(7)	166.11(3)	96.61(3)	96.80(3)	175.71(8)
[PNP]NiBr, 15	83.77(11)	83.15(11)	166.30(5)	97.20(4)	96.15(4)	175.69(11)
[PNP]NiI, 16	83.14(10)	83.82(10)	166.43(5)	95.92(4)	97.41(4)	174.85(10)

confirms the presence of two different environments for the phosphorus atoms as suggested by the ^1H NMR spectrum.

Using a single crystal obtained from a solution of **12** in toluene upon layering with petroleum ether, we determined the structure of complex **12** by the X-ray diffraction method. ORTEP diagrams along with selected bond lengths and angles, and the refinement data are given in Figure 4 and Table 1,

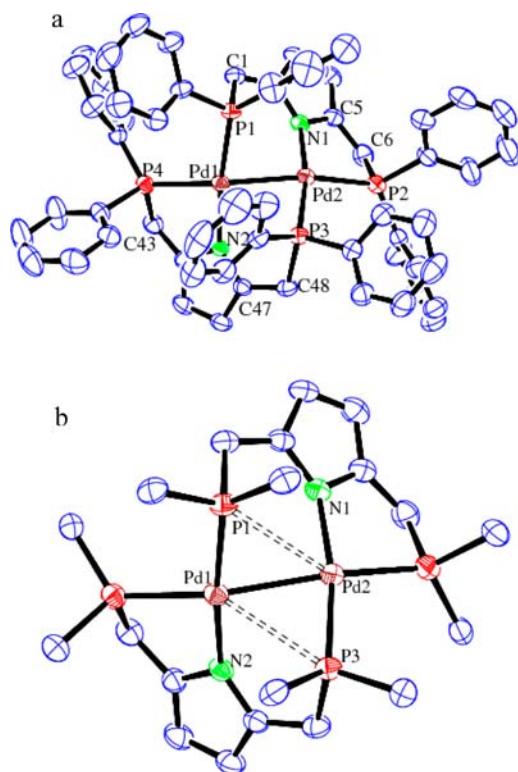


Figure 4. ORTEP diagram of $12 \cdot 0.5(\text{C}_6\text{H}_6)$ with 30% probability ellipsoids: view b is showing the existence of the weak interactions between the diagonally positioned P and Pd atoms. All H atoms, the lattice benzene molecule, and the phenyl carbon atoms except the *ipso* carbons (view b) are omitted for clarity. Selected bond lengths (Å) and angles (deg): Pd1–Pd2 2.5470(5), N1–Pd2 2.111(4), N2–Pd1 2.090(4), P1–Pd1 2.2395(13), P2–Pd2 2.3504(14), P3–Pd2 2.2329(13), P3–Pd1 2.9744(14), P4–Pd1 2.3559(14), N2–Pd1–P1 171.32(11), N2–Pd1–P4 81.26(11), P1–Pd1–P4 104.09(5), N2–Pd1–Pd2 92.58(10), P1–Pd1–Pd2 79.84(4), P4–Pd1–Pd2 156.85(4), N2–Pd1–P3 72.26(11), P1–Pd1–P3 104.85(4), P4–Pd1–P3 146.67(4), Pd2–Pd1–P3 46.92(3), N1–Pd2–P3 169.58(11), N1–Pd2–P2 82.79(12), P3–Pd2–P2 106.38(5), N1–Pd2–Pd1 93.03(11), P3–Pd2–Pd1 76.65(4), P2–Pd2–Pd1 159.44(4).

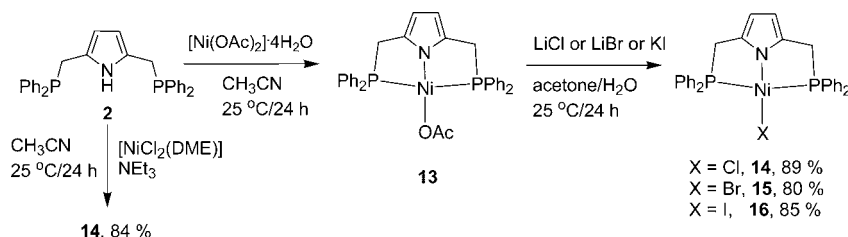
respectively. The X-ray structure revealed that the binuclear complex consists of two Pd(I) centers bridged by two anionic PNP pincer ligands coordinated in a $\kappa^2\text{PN}, \kappa^1\text{P}$ bonding modes in a sort of trans fashion. In the structure, each ligand is twisted and forms two different rings: a puckered five-membered chelate ring and a puckered six-membered ring with the two Pd centers. The six-membered Pd1–P1 and Pd2–P3 bond distances (2.2395 Å and 2.2329 Å) are shorter than the chelate five-membered Pd1–P4 and Pd2–P2 bond distances (2.3559 Å and 2.3504 Å). The short Pd1–P1 and Pd2–P3 bonds which are trans to the pyrrolide N atoms can be attributed to the weaker trans influence of the pyrrolide N, while the long Pd–P bonds which are trans to the Pd–Pd bond can be because of

the stronger trans influence of the Pd–Pd bond.³⁵ The geometry around each metal center is distorted square planar. For example, around the Pd1 center, while P1 and N2 are almost linear (N2–Pd1–P1 = 171.32°), P4 and Pd2 deviate considerably from the linearity (P4–Pd1–Pd2 = 156.85°). The two Pd square planes are twisted probably owing to the steric repulsion between the two ligands which forms $\kappa^2\text{PN}, \kappa^1\text{P}$ bonding modes with the dihedral angles: N2–Pd1–Pd2–P3 = –62.64° and N1–Pd2–Pd1–P1 = –59.81°. The Pd–Pd bond distance of 2.5470 Å indicates a σ -bond between the two Pd(I) centers. The observed Pd–Pd distance is close to the values (2.55 to 2.56 Å)^{35,36} but is longer than the values (2.41 to 2.50 Å)³⁷ reported for the dinuclear Pd(I) complexes containing both chelate and bridging modes of pincer ligands. Additionally, this observed Pd–Pd distance is shorter than those (2.57³⁸ and 2.61 Å³⁹) found in complexes containing an unbridged Pd(I)–Pd(I) bond. Interestingly, two short contacts are observed within the two six-membered rings: P3...Pd1 = 2.974 Å and P1...Pd2 = 3.081 Å. These distances are considerably shorter than 3.45 Å, the sum of the van der Waals radii of P (1.85 Å) and Pd (1.60 Å) atoms,⁴⁰ and hence indicate the existence of weak bonding interactions between the diagonally positioned P and Pd atoms in each six-membered ring, which is facilitated by the twisted square planes of the two Pd centers.

Although complex **12** is expected to be relatively more stable because of the presence of both the chelating and the bridging modes of the pincer ligand, it readily undergoes a transformation in CDCl_3 to give rise to complex **10** as shown by the ^1H and ^{31}P NMR spectra. To confirm the transformation of complex **12** to **10**, variable temperature ^1H NMR experiments were carried out using crystals of **12** in CDCl_3 . The VT ^1H NMR spectra showed the gradual appearance of a triplet at $\delta = 3.87$ ppm, which is the same signal obtained for the PCH_2 groups of complex **10**, along with the resonances corresponding to complex **12**, upon gradually increasing the temperature of the sample to 60 °C (see the Supporting Information, Figure S64). In addition, the ^{31}P NMR spectrum of **12** in CDCl_3 also showed signals corresponding to both the complexes after few hours (see the Supporting Information, Figure S65), supporting the transformation of complex **12** to **10**. This conversion is almost over within 2 days at room temperature as shown by the ^1H NMR spectrum. Thus, the Pd(I) complex **12** is not stable and transforms into the mononuclear Pd(II) chloride complex **10** in CDCl_3 probably via oxidative addition reactions. Conversely, **12** does not change to **10** in $\text{DMSO}-d_6$ after 24 h as shown by the ^{31}P NMR spectra recorded at different intervals, suggesting that the complex is stable in this coordinating solvent. This prompted us to carry out the reaction in CDCl_3 to see if complex **10** is formed or not. Indeed, the characteristic triplet of the methylene protons of complex **10** is found as a sole product in the ^1H NMR spectrum recorded for a reaction between **2** and $[\text{Pd}_2(\text{dba})_3] \cdot \text{CHCl}_3$ in CDCl_3 carried out in a NMR tube. Besides, this transformation explains why complex **12** was isolated in low yield (23%) given the presence of CHCl_3 in the starting material Pd(0) complex.

Synthesis and Characterization of Ni Complexes. The reaction between an equimolar quantity of the PNP pincer ligand **2** and $[\text{Ni}(\text{OAc})_2] \cdot 4\text{H}_2\text{O}$ gave a mixture of two products in approximately 4:1 ratio as shown by the ^{31}P NMR and ^1H spectra in CDCl_3 . The ^{31}P NMR spectrum shows two singlets: one at δ 27.0 (major) and the other at δ 30.8 ppm (minor). The signal at δ 27.0 ppm is assigned to complex **13** (see Scheme 4) because the other Ni(II) complexes **14–16**, which

Scheme 4. Synthesis of Ni(II) Complexes 13–16 Bearing the PNP Pincer Ligand 2



give singlets in this region, were synthesized in very good yields without separation of complex 13 from the mixture (see below). Complex 13 gives the characteristic triplet for the methylene protons in the ^1H spectrum, which is supported by the ^{13}C NMR spectrum showing a triplet owing to the $J(\text{C},\text{P})$ coupling for the methylene carbon atoms. The IR spectrum shows a CO stretching frequency at 1625 cm^{-1} for the presence of an acetate group in the structure of 13. In addition, the HRMS(ESI+) spectrum shows a peak m/z at 561.0298 (calcd 561.0688) corresponding to the $[\text{M}-\text{OAc}+2\text{H}^++\text{K}^+]^{4+}$ ion. These data support the structure proposed for the mononuclear Ni(II) complex 13 containing the monoanionic tridentate pincer ligand 2 and one acetate group as shown in Scheme 4.

Without separating complex 13, the reaction mixture was treated with an excess of LiCl or LiBr or KI in acetone/water at room temperature to give the corresponding halide ion substituted mononuclear Ni complexes 14–16 in good yields (80–89%) (see Scheme 4). These products are formed via the acetate-halide ion exchange reaction in an aqueous–organic medium. Alternatively, complex 14 was synthesized by the reaction of $[\text{NiCl}_2(\text{DME})]$ with 2 in the presence of 1 equiv of Et_3N in 84% yield. All the three Ni halide pincer complexes were characterized by spectroscopic and single crystal X-ray diffraction studies. While the ^1H NMR spectra of the Ni(II) pincer complexes 13–16 remain similar to each other; all displayed a virtual triplet for the methylene protons and a singlet for the pyrrole β -CH protons, different singlets at $\delta = 27.0, 30.6, 35.0, 42.6$ ppm for 13, 14, 15, and 16, respectively, are observed in their ^{31}P NMR spectra. As can be noticed, the phosphorus chemical shift moves toward the deshielded region as the electronegativity of the trans group attached to the Ni center decreases, $\text{Cl} > \text{Br} > \text{I}$.

The X-ray structures of 14, 15, and 16 are depicted in Figures 5, 6, and 7, respectively, and their selected bond lengths and angles are given in Table 2. Complexes 14, 15, and 16 exhibit very similar unit cell parameters and have the same space group $P2_1/c$ (Table 1). The structures of these complexes resemble the structure of the Pd(II) complex 10. In each structure, the pincer ligand is slightly twisted and adopts the $\text{mer-}\kappa^3\text{-PNP}$ coordination mode resulting in two fused five-membered chelate rings with the Ni(II) center with the dihedral angles given below each diagram. A distorted square planar geometry was observed in each Ni(II) complex as indicated by their bond angles. As can be observed from Table 2, both the $\text{N}-\text{Ni}-\text{P1}$ and $\text{N}-\text{Ni}-\text{P2}$ bond angles are lower than the other two angles, $\text{P1}-\text{Ni}-\text{X}$ and $\text{P2}-\text{Ni}-\text{X}$ ($\text{X} = \text{Cl}, \text{Br}, \text{and I}$). In addition, the $\text{P1}-\text{Ni}-\text{P2}$ angles ($\sim 166^\circ$), a considerably lower value compared to the expected 180° , are lower than the $\text{N}-\text{Ni}-\text{X}$ angles ($\sim 175^\circ$). These are typically observed values for a distorted square planar Ni(II) pincer complex containing two fused five-membered chelate rings and

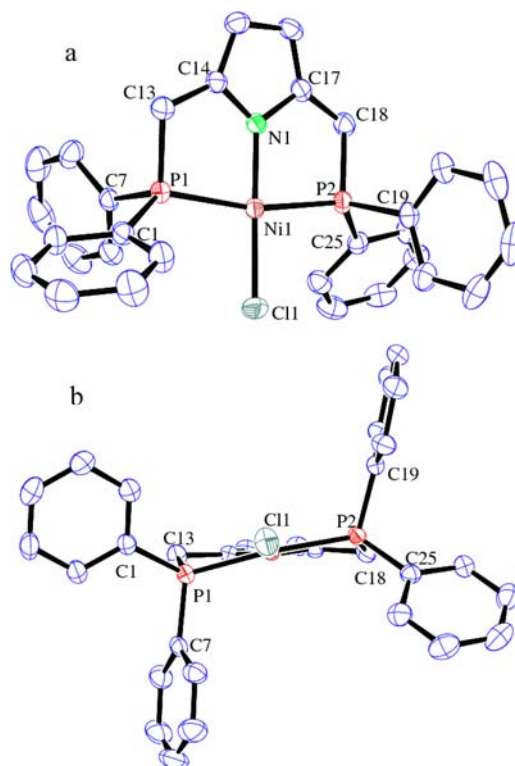


Figure 5. ORTEP diagram of the nickel chloride complex 14 (30% thermal ellipsoids): (a) top view, and (b) side view, showing the twisted arrangement of the pincer ligand. All hydrogen atoms are omitted for clarity. Selected torsion angles: $\text{P1}-\text{Ni}-\text{N}-\text{C14} = 15.85^\circ$; $\text{P2}-\text{Ni}-\text{N}-\text{C17} = 2.16^\circ$.

are attributed to the tridentate $\text{mer-}\kappa^3\text{-PNP}$ coordination mode that is forcefully adopted by the pincer ligand 2.^{18b,20c,32,41}

In the structure of complex 14, the Ni–Cl bond distance is $2.1699(9)\text{ \AA}$ which is shorter than those (2.232 \AA ,³² and 2.2167 \AA ,^{18b}) found in the analogous Ni(II) complexes formed by the PCP and the PCN pincer ligands, respectively. This is attributed to the weaker trans influence of pyrrolide N atom as observed in the Pd complex 10. However, the observed Ni–N and Ni–P bond distances fall in the range reported for the analogous Ni(II) complexes bearing the PNP pincer ligand.^{42,29}

In the structure of complex 15, while the Ni–P bond distances ($2.2085(13)\text{ \AA}$ and $2.1988(13)\text{ \AA}$) are close to the reported Ni–P bond distance (2.183 \AA), the Ni–N bond distance ($1.856(3)\text{ \AA}$) is shorter than the Ni–N bond distance (1.912 \AA) reported for an analogous “(PNP)NiBr” pincer complex⁴² containing an amide bond, indicating that the Ni–N bond in complex 15 is stronger because of the pyrrolide nitrogen.

In the structure of complex 16, the Ni–N and Ni–P bond distances are very similar to those found in the structures of 14

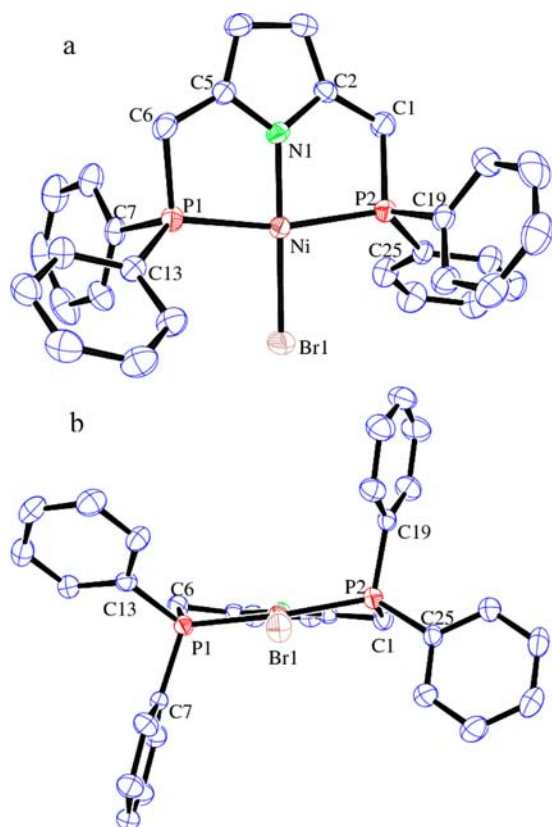


Figure 6. ORTEP diagram of the nickel bromide complex **15** (30% thermal ellipsoids): (a) top view, and (b) side view, showing the twisted arrangement of the pincer ligand. All hydrogen atoms are omitted for clarity. Selected torsion angles: P1–Ni–N–C5 = 3.09°; P2–Ni–N–C2 = 15.24°.

and **15**. However, as observed in the chloride and bromide complexes, the Ni–I bond distance of 2.4844(7) Å is shorter than the distance of 2.5229(9) Å found in the structure of [Ni{2,6-(CH₂PⁱPr₂)₂-C₆H₃}] in which the iodide atom is trans to the more trans influencing carbon atom.⁴³

DFT Study. DFT calculations are performed to understand the nature of the weak interaction between the diagonally oriented Pd and P atoms in the structure of complex **12**. From the DFT calculations, this interaction is shown to be through the responsible donor and acceptor molecular orbitals (see the Supporting Information, Table 3). The HOMO-15 and HOMO-16 (Figure 8) are involved in the electron delocalization for these interactions, as shown in the simplified MO interaction diagram (Figure 9). Wiberg bond indices for these weak interactions are 0.2507 and 0.2275 which are considerably lower than those (0.5575 and 0.4869) obtained for the normal bonds existing between the Pd and P atoms in the same structure. This supports the weak bonding interactions as observed in the crystal structure of complex **12**.

CONCLUSION

In conclusion, a new synthetic method was developed for the preparation of a novel class of pyrrole-based PNP pincer and dipyrrolylmethane-based PNNP type ligands from the double Mannich bases of the corresponding pyrrole systems in high yields. The coordination chemistry of the PNP pincer ligand was explored with the synthesis of a series of mononuclear Ni(II) and Pd(II), and dinuclear Pd(I) complexes. The

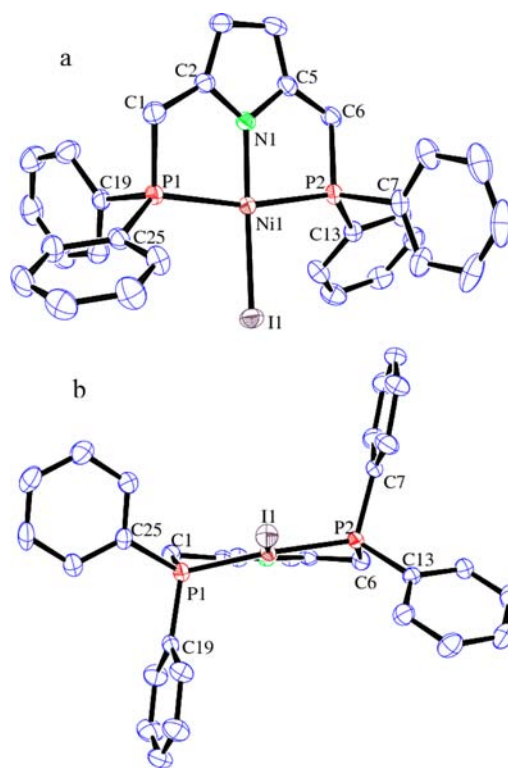


Figure 7. ORTEP diagram of the nickel iodide complex **16** (30% thermal ellipsoids): (a) top view, and (b) side view, showing the twisted arrangement of the pincer ligand. All hydrogen atoms are omitted for clarity. Selected torsion angles: P1–Ni–N–C2 = 14.90°; P2–Ni–N–C5 = 4.80°.

formation of Pd(I) dimer complex **12** is solvent dependent. The bonding modes of the pincer ligand in these complexes, bridging and chelating, were established by the X-ray diffraction method, which demonstrated the versatile nature of the pincer ligand. The conversion of the dimeric Pd(I) complex to the mononuclear Pd(II) complex was demonstrated by ¹H and ³¹P NMR methods. The weak interactions present in the crystal structure of the Pd(I) dimer were analyzed by DFT calculations. Synthesis of other phosphine ligands using this method, and synthesis and catalysis studies of other metal complexes are in progress in our laboratory.

EXPERIMENTAL SECTION

General Procedure. All reactions and manipulations were carried out under a nitrogen atmosphere using standard Schlenk-line techniques. Petroleum ether (bp 40–60 °C) and other solvents were distilled according to the standard procedures. 2,5-Bis(dimethylaminomethyl)pyrrole **1**,⁴⁴ 1,9-bis(*N,N*-dimethylaminomethyl)dipyrrolylmethane **4**,⁴⁵ [Pd₂(dba)₃]·CHCl₃,⁴⁶ [Pd(COD)Cl₂],⁴⁷ [Pd(PhCN)₂Cl₂],⁴⁸ [NiCl₂(DME)],⁴⁹ and Ph₂PH⁵⁰ were prepared as reported. Other chemicals were obtained from commercial sources and were used without further purification. ¹H NMR (200 and 400 MHz), ¹³C NMR (50.3 and 100.6 MHz), and ³¹P (161.9 MHz) spectra were recorded on Bruker ACF200 and AV400 spectrometers at room temperature. ¹H NMR chemical shifts are referenced with respect to the chemical shift of the residual protons present in the deuterated solvents. For ³¹P NMR measurements 85% H₃PO₄ as an external standard was used. FTIR spectra were recorded using Perkin–Elmer Spectrum Rx. Elemental analyses were carried out using a Perkin–Elmer 2400 CHN analyzer. High Resolution Mass Spectra (ESI) were recorded using an LCT Orthogonal Acceleration TOF Electrospray Mass Spectrometer.

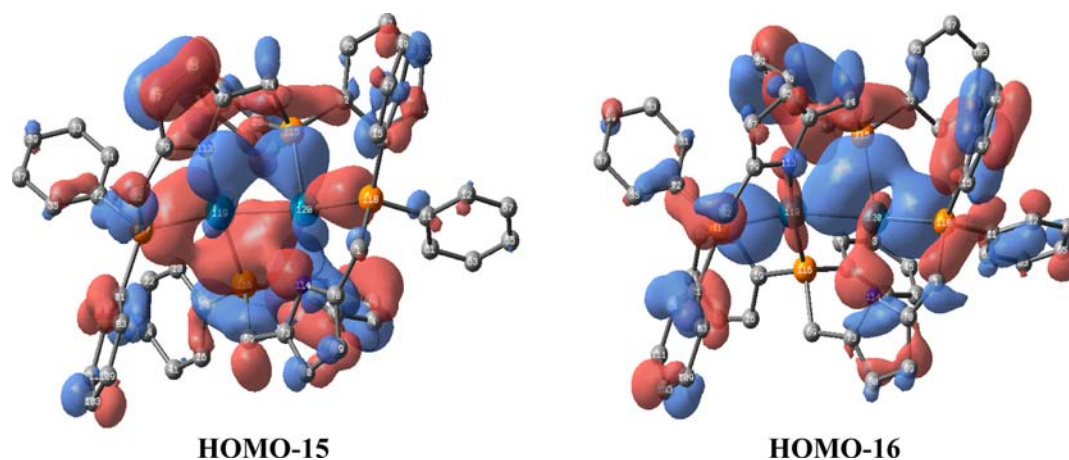


Figure 8. Selected occupied molecular orbitals for the weak interactions in the structure of complex 12.

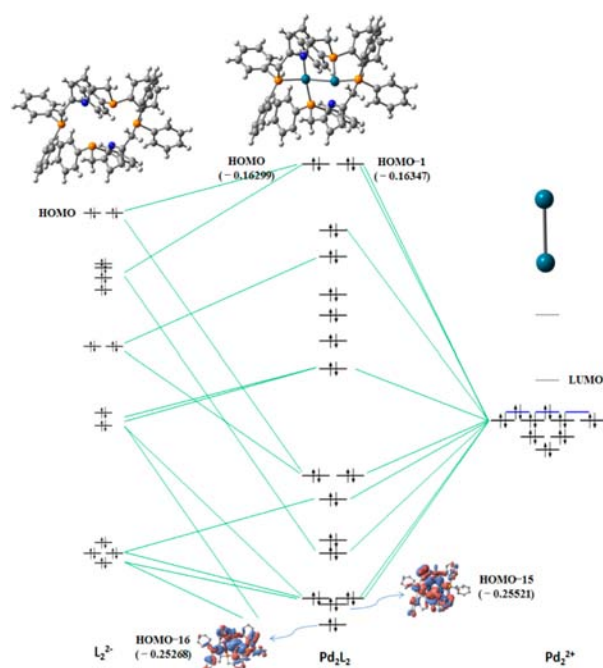


Figure 9. Simplified interaction MO diagram showing the selected energy levels and their interactions including the weak interactions in the structure of complex 12.

Computational Details. Geometry optimization (B3LYP/LANL2DZ) and frequency calculation are performed using Gaussian 09 program package.⁵¹ The Wiberg bond indices of complex 12 are calculated by NBO at the B3LYP/LANL2DZ level. The molecular orbitals are generated by using GaussView, Version 3.0.⁵² The interaction MO diagram was generated by using the ADF program⁵³ following the work of Vega et al.⁵⁴ Calculation is carried out using local density approximation with gradient corrections for exchange (Becke88)⁵⁵ and correlation (Perdew).⁵⁶ The standard ADF basis set is used for all the atoms in the complex along with the ZORA scalar Hamiltonian.⁵⁷ Fragment interaction analysis between L_2^{2-} and Pd_2^{2+} is done through a single point calculation using the method proposed by Ziegler to generate the interaction diagram.⁵⁸ Using this approach, the orbital interaction energies are decomposed into components related to various irreducible representations. As the system is too large it is difficult to generate the exact nature of the irreducible representations. The geometrical parameters, comparison of selected bond lengths and bond angles with those obtained by the X-ray diffraction method, and Wiberg bond indices are given in the Supporting Information.

Synthesis of 2,5-Bis(diphenylphosphinomethyl)pyrrole, 2. A mixture of 2,5-bis(dimethylaminomethyl)pyrrole (6.0 g, 33.09 mmol) and Ph_2PH (12.32 g, 66.17 mmol) was heated to 150 °C with stirring for 22 h. The reaction mixture was cooled to room temperature, giving a sticky precipitate which was dissolved in 40 mL of toluene. To this solution was added petroleum ether (120 mL) and then cooled to -10 °C to give a colorless precipitate of 2 after 3 days. The precipitate was separated and dried under vacuum (13.8 g, 29.7 mmol, 90% yield). 1H NMR ($CDCl_3$, 400 MHz, ppm): δ = 3.30 (s, 4H, CH_2), 5.66 and 5.67 (s, 2H, pyrrole β -CH), 7.33 (br m, 20H, phenyl CH), 7.67 (br s, 1H, NH). $^{31}P\{^1H\}$ NMR (161.9 MHz, $CDCl_3$, ppm): δ = -16.3 (s). ^{13}C NMR ($CDCl_3$, 50.3 MHz, ppm): δ = 28.2 (d, $J(C,P)$ = 15.1 Hz, CH_2), 107.6 (d, $J(C,P)$ = 5 Hz, pyrrole β -CH), 126.2 (d, $J(C,P)$ = 10 Hz, pyrrole α -C), 128.5, 128.6, 128.7, 128.9, 132.7, 133.1, 138.2, 138.5 (phenyl C). FT-IR (KBr, cm^{-1}): ν = 3364 (w), 3050 (w), 2867 (w), 1645 (w), 1580 (w), 1480 (w), 1430 (m), 1400 (w), 1306 (w), 1269 (w), 1205 (w), 1096 (w), 1028 (w), 975 (w), 834 (w), 808 (w), 775 (w), 740 (s), 694 (s), 638 (w), 503 (m), 475 (w), 446 (w). Anal. Calcd. for $C_{30}H_{27}NP_2$: C, 77.74; H, 5.87; N, 3.02. Found: C, 77.17; H, 5.95; N, 2.98.

Synthesis of 1,9-Bis(diphenylphosphinomethyl)dipyrrolylmethane, 5. A solution of 1,9-bis(*N,N*-dimethylaminomethyl)dipyrrolylmethane, 4 (6.0 g, 14.55 mmol) and Ph_2PH (5.69 g, 30.55 mmol) in toluene (15 mL) was heated to 110 °C with stirring for 20 h. The reaction mixture was cooled to room temperature and then the solvent was removed under vacuum. The resultant sticky precipitate was dissolved in 40 mL of toluene to which petroleum ether (120 mL) was added and cooled to -10 °C to give colorless precipitate of 5 after 3 days. The colorless precipitate was separated and dried under vacuum (9.3 g, 13.4 mmol, 92% yield). Suitable single crystals of 5 were obtained from CH_2Cl_2 and petroleum ether mixture (1:2). 1H NMR ($CDCl_3$, 400 MHz, ppm): δ = 3.38 (s, 4H, CH_2), 5.66 (t, 2H, pyrrole β -CH), 5.85 (t, 2H, pyrrole β -CH), 6.92–6.97 (m, 4H, phenyl CH), 7.23–7.45 (m, 26H, phenyl CH), δ 7.53 (br s, 2H, NH). $^{31}P\{^1H\}$ NMR (161.9 MHz, $CDCl_3$, ppm): δ = -15.5 (s). ^{13}C NMR ($CDCl_3$, 100.6 MHz, ppm): δ = 28.1 (d, $J(C,P)$ = 14.6 Hz, CH_2), 55.9 (s, *meso* C), 107.1 (d, $J(C,P)$ = 5.7 Hz, pyrrole β -CH), 110.0 (s, pyrrole β -CH), 126.8 (t, $J(C,P)$ = 7.4 Hz, pyrrole α -C), 127.9 (s, pyrrole α -C), 128.7, 128.9, 128.9, 129.0, 129.2, 129.4, 129.5, 131.1, 131.2, 132.9, 133.0, 134.4, 134.4, 138.2, 138.4, 146.1 (phenyl C). FT-IR (KBr, cm^{-1}): ν = 3415 (m), 3049 (w), 1955 (w), 1880 (w), 1818 (w), 1574 (w), 1483 (w), 1433 (m), 1410 (w), 1263 (w), 1178 (w), 1097 (m), 1042 (m), 825 (w), 776 (m), 738 (s), 697 (s), 625 (w), 509 (w), 474 (w), 429 (w). Anal. Calcd. for $C_{47}H_{40}N_2P_2$: C, 81.25; H, 5.80; N, 4.03. Found: C, 80.90; H, 6.00; N, 3.88.

Synthesis of 2,5-Bis(diphenylphosphorylmethyl)pyrrole, 6. To a toluene (10 mL) solution of 2 (0.10 g, 0.215 mmol) was added aqueous H_2O_2 (0.2 mL, 1.72 mmol, 30%). The solution was stirred for overnight to give colorless precipitate of compound 6 which was

separated and dried under vacuum (0.093 g, 0.17 mmol, 80% yield). Suitable single crystals were obtained by slow evaporation of a solution of **6** in CH₂Cl₂/petroleum ether (v/v 1:3). ¹H NMR (CDCl₃, 200 MHz, ppm): δ = 3.63 (d, 4H, ²J(P,H) = 11.4 Hz, CH₂), 5.55 (s, 2H, pyrrole β-CH), 7.37–7.69 (m, 20H, phenyl CH), 10.15 (s, 1H, NH). ³¹P{¹H}NMR (161.9 MHz, CDCl₃, ppm): δ = 31.5(s). ¹³C NMR (CDCl₃, 50.3 MHz, ppm): δ = 30.7 (d, J(C,P) = 69.4 Hz, CH₂), 108.9 (s, pyrrole β-CH), 121.2 (s, pyrrole α-C), 128.7, 128.8, 128.9, 130.4, 131.2, 131.3, 131.3, 132.3 (phenyl C). FT-IR (KBr, cm⁻¹): ν = 3475 (s), 3373 (s), 3204 (m), 2902 (w), 1644 (w), 1586 (w), 1486 (w), 1435 (m), 1390 (w), 1312 (w), 1171 (s), 1121 (m), 1029 (w), 990 (w), 827 (m), 744(m), 730 (m), 696 (s), 531 (s). HRMS (+ESI): Calcd *m/z* for [M + H]⁺ C₃₀H₂₈NP₂O₂: 496.1595, Found: 496.1647.

Synthesis of 2,5-Bis(diphenylthiophosphorylmethyl)pyrrole, 7. To a toluene (10 mL) solution of **2** (0.10 g, 0.215 mmol) was added elemental sulfur (0.0172 g, 0.537 mmol). The solution was stirred for overnight and then the solvent was removed under vacuum. The resultant residue was washed with petroleum ether (2 × 50 mL) and then dried under vacuum to give **7** (0.095 g, 0.18 mmol, 84% yield). ¹H NMR (CDCl₃, 200 MHz, ppm): δ = 3.79 (d, 4H, ²J(P,H) = 11.4 Hz, CH₂), 5.62 (s, 2H, pyrrole β-CH), 7.36–7.51 (m, 12H, phenyl CH), 7.67–7.77 (m, 8H, phenyl CH), 9.44 (s, 1H, NH). ³¹P{¹H}NMR (161.9 MHz, CDCl₃, ppm): δ = 38.8(s). ¹³C NMR (CDCl₃, 50.3 MHz, ppm): δ = 34.5 (d, J(C,P) = 55.3 Hz, CH₂), 109.6 (s, pyrrole β-CH), 121.7(s, pyrrole α-C), 128.5, 128.6, 128.7, 128.8, 131.4, 131.5, 131.6, 131.7, 131.8, 133.0 (phenyl C). FT-IR (KBr, cm⁻¹): ν = 3354 (w), 3048 (w), 2891 (w), 1644 (w), 1580 (w), 1485 (w), 1434 (m), 1387 (w), 1306 (w), 1264 (w), 1172 (w), 1102 (s), 1035 (w), 996 (w), 814 (w), 778 (w), 743 (m), 693 (s), 601 (m), 506 (m). HRMS (+ESI): Calcd *m/z* for [M+2H]²⁺ C₃₀H₂₉NP₂S₂: 529.1217, Found: 529.1201.

Synthesis of 1,9-Bis(diphenylphosphorylmethyl)diphenyldipyrrolylmethane, 8. To a toluene (10 mL) solution of **5** (0.150 g, 0.216 mmol) was added aqueous H₂O₂ (0.2 mL, 1.72 mmol, 30%). The solution was stirred for overnight. After separating the toluene layer from the aqueous layer, toluene was removed under vacuum. The resultant residue was washed with petroleum ether (2 × 50 mL) and dried under vacuum to give **8** (0.117 g, 0.16 mmol, 74% yield). ¹H NMR (CDCl₃, 200 MHz, ppm): δ = 3.68 (d, 4H, ²J(P,H) = 12.4 Hz, CH₂), 5.62 (s, 2H, pyrrole β-CH), 5.71 (s, 2H, pyrrole β-CH), 6.91–7.70 (m, 30H, phenyl CH), 8.93 (br s, 2H, NH). ³¹P{¹H}NMR (161.9 MHz, CDCl₃, ppm): δ = 31.6(s). ¹³C NMR (CDCl₃, 50.3 MHz, ppm): δ = 30.4 (d, J(C,P) = 69.9 Hz, CH₂), 56.0 (s, meso C) 108.3 (s, pyrrole β-CH), 110.1(s, pyrrole β-CH), 120.4 (s, pyrrole α-C), 120.6 (s, pyrrole α-C), 127.7, 128.2, 128.4, 128.6, 128.8, 129.6, 130.2, 130.9, 131.1, 131.3, 131.5, 132.0, 132.6, 132.9, 136.2, 145.8 (phenyl C). FT-IR (KBr, cm⁻¹): ν = 3282 (m), 3053 (m), 2946 (w), 2889 (w), 1710 (m), 1639 (w), 1592 (w), 1488 (w), 1436 (s), 1315 (w), 1172 (s), 1123 (s), 1028 (w), 823 (w), 793 (m), 732 (s), 695 (s), 632 (w), 537 (s). HRMS (+ESI): Calcd *m/z* for [M+H]⁺ C₄₇H₄₁N₂P₂O₂: 727.2643, Found: 727.3982.

Synthesis of 1,9-Bis(diphenylthiophosphorylmethyl)diphenyldipyrrolylmethane, 9. To a toluene (10 mL) solution of **5** (0.150 g, 0.216 mmol) was added elemental sulfur (0.0172 g, 0.537 mmol). The solution was stirred overnight. The solvent was removed under vacuum to give a residue which was washed with petroleum ether and dried under vacuum to give **9** (0.120 g, 0.16 mmol, 73% yield). ¹H NMR (CDCl₃, 200 MHz, ppm): δ = 3.89 (d, 4H, ²J(P,H) = 12.4 Hz, CH₂), 5.73 (br s, 2H, pyrrole β-CH), 5.78 (br s, 2H, pyrrole β-CH), 7.05–7.85 (m, 30H, phenyl CH), 8.84 (br s, 2H, NH). ³¹P{¹H}NMR (161.9 MHz, CDCl₃, ppm): δ = 39.3(s). ¹³C NMR (CDCl₃, 50.3 MHz, ppm): δ = 34.2 (d, J(C,P) = 54.3 Hz, CH₂), 56.0 (s, meso C), 109.1 (d, J(C,P) = 7 Hz, pyrrole β-CH), 109.8 (s, pyrrole β-CH), 120.7 (d, J(C,P) = 8 Hz, pyrrole α-C), 126.7(s, pyrrole α-C), 127.9, 128.4, 128.6, 128.8, 129.2, 129.6, 131.5, 131.7, 133.0, 135.9, 145.9 (phenyl CH). FT-IR (KBr, cm⁻¹): ν = 3417 (w), 3348 (w), 3052 (w), 2880 (w), 1813 (w), 1574 (w), 1484 (m), 1435 (s), 1387 (w), 1261 (w), 1180 (m), 1103 (s), 1042 (m), 821 (m), 779 (m), 744 (w), 696 (s), 638 (w), 602 (m), 506 (s). HRMS (+ESI): Calcd *m/z* for [M+H]⁺ C₄₇H₄₁N₂P₂S₂: 759.2186, Found: 759.2631.

Synthesis of [PdCl₂(C₄H₂N-2,5-(CH₂PPh₂)₂-κ³PNP]], 10. To a mixture of [PdCl₂(PhCN)₂] (0.100 g, 0.260 mmol) and **2** (0.121 g, 0.260 mmol) in acetonitrile (15 mL) was added dropwise triethylamine (0.080 mL, 0.573 mmol) with stirring at room temperature. After 24 h stirring, the solvent was removed under vacuum, and the residue was dissolved in dichloromethane. The dichloromethane solution was washed with water (3 × 30 mL) and dried over anhydrous Na₂SO₄. The solution was filtered, and the solvent was removed under vacuum to give a light brown precipitate of **10** (0.137 g, 0.23 mmol, 87% yield). Suitable single crystals were obtained from a solution of **10** in toluene at -18 °C. ¹H NMR (CDCl₃, 200 MHz, ppm): δ = 3.87 (t, 8H, ²J(P,H) = 5 Hz, CH₂), 6.09 (s, 4H, pyrrole β-CH), 7.40–7.46 (m, 24H, phenyl CH), 7.81–7.91 (m, 16H, phenyl CH). ³¹P{¹H}NMR (161.9 MHz, CDCl₃, ppm): δ = 33.8(s). ¹³C NMR (CDCl₃, 100.6 MHz, ppm): δ = 34.0 (t, J(C,P) = 13.5 Hz, CH₂), 104.8 (t, J(C,P) = 7 Hz, pyrrole β-CH), 129.1, 129.2, 129.2 (phenyl C), 130.4 (s, pyrrole α-C), 130.9, 131.1, 131.2, 131.3, 133.0, 133.1, 133.1, 136.1, 136.2 (phenyl C). FT-IR (KBr, cm⁻¹): ν = 3052 (w), 1616 (w), 1482 (w), 1433 (s), 1374 (w), 1311 (w), 1262 (w), 1103 (s), 998 (w), 832 (w), 740 (s), 691 (s), 516 (s), 478 (m). HRMS (+ESI): Calcd *m/z* for [M-Cl⁻+K⁺]²⁺ C₃₀H₂₆NP₂PdK: 607.0212, Found: 607.0836.

Synthesis of [Pd₂Cl₄{μ-C₄H₃N-2,5-(CH₂PPh₂)₂-κ²PP]₂], 11. To a toluene (10 mL) solution of [PdCl₂(PhCN)₂] (0.05 g, 0.130 mmol) was added **2** (0.06 g, 0.130 mmol). The solution was stirred for overnight at room temperature. The solvent was removed under vacuum to give a residue which was washed with petroleum ether and dried under vacuum to give **11** as a yellow precipitate (0.079 g, 0.06 mmol, 95% yield). ¹H NMR (CDCl₃, 400 MHz, ppm): δ = 3.83 (br s, 8H, CH₂), 5.06 (s, 4H, pyrrole β-CH), 7.24–7.64 (m, 40H, phenyl CH), 9.86 (br s, 2H, NH). ³¹P{¹H}NMR (161.9 MHz, CDCl₃, ppm): δ = 14.3(s). ¹³C NMR (CDCl₃, 100.6 MHz, ppm): 26.8 (s, CH₂), 109.1 (s, pyrrole β-CH), 122.2 (s, pyrrole α-C), 128.4, 129.8, 130.0, 130.3, 130.8, 131.0, 133.9, 134.3 (phenyl C). FT-IR (KBr, cm⁻¹): ν = 3344(m), 3048 (m), 1583 (w), 1480 (m), 1434(s), 1390 (m), 1309 (w), 1273 (w), 1178 (m), 1102 (s), 1035 (m), 996 (w), 812 (m), 772 (m), 743 (s), 692 (s), 641 (w), 504 (m). Anal. Calcd. for C₆₀H₅₄Cl₄N₂P₄Pd₂: C, 56.23; H, 4.25; N, 2.19. Found: C, 55.83; H, 4.39; N, 2.13. HRMS (+ESI): Calcd *m/z* for [M-3Cl⁻]³⁺ C₆₀H₅₄ClN₂P₄Pd₂: 1173.0996, Found: 1173.9480 and Calcd *m/z* for [M-4Cl⁻+K⁺]⁵⁺ C₆₀H₅₄KN₂P₄Pd₂: 1177.0944, Found: 1177.9426.

Synthesis of [Pd₂{μ-C₄H₂N-2,5-(CH₂PPh₂)₂-κ²PN,κ¹P]₂], 12. To a toluene (15 mL) solution of [Pd₂(dba)₃]·CHCl₃ (0.15 g, 0.145 mmol) was added **2** (0.154 g, 0.330 mmol). The solution was stirred for 16 h at room temperature. The solvent was removed under vacuum. The resultant residue was washed with petroleum ether (2 × 10 mL) followed by washing with diethyl ether (1 × 10 mL). The residue was dissolved in 20 mL of toluene of which petroleum ether was added slowly to form a layer. Red crystals of compound **12** were formed after 3 weeks. The crystals were separated, washed with petroleum ether and then dried under vacuum (0.04 g, 0.034 mmol, 23.5% yield). ¹H NMR (CDCl₃, 400 MHz, ppm): δ = 4.05 and 3.53 (ABX spin system, 4H, ²J(H_A,H_B) = 16.6 Hz, ²J(P,H_A) and ²J(P,H_B) = 7.2 Hz, PCH₂), 3.72 and 3.46 (ABX spin system, 4H, ²J(H,H) = 15.2 Hz, ²J(P,H) = 7.0 Hz, PCH₂), 6.02 (s, 2H, pyrrole β-CH), 6.15 (s, 2H, pyrrole β-CH), 6.81–7.42 (m, 40H, phenyl CH). ³¹P{¹H}NMR (161.9 MHz, CDCl₃, ppm): δ = 20.5(s) and 17.6(s). ¹³C NMR (CDCl₃, 100.6 MHz, ppm): δ = 30.6 (d, J(C,P) = 33.3 Hz, CH₂), 35.9 (t, J(C,P) = 10.4 Hz, CH₂), 104.8 (d, J(C,P) = 230.5 Hz, pyrrole β-CH), 106.0 (d, J(C,P) = 7.7 Hz, pyrrole β-CH), 125.3 (d, J(C,P) = 12.8 Hz, pyrrole α-C), 127.4, 127.5, 127.6, 127.7, 127.9, 127.9, 128.0, 128.0, 128.1, 128.2, 128.3, 128.6, 128.7, 128.8, 128.9, 129.0, 129.7, 130.5, 130.9,131.0, 131.1, 131.1, 131.2, 131.8, 131.9, 132.6, 132.8, 132.9, 133.1, 133.2, 133.3, 133.4, 133.5, 133.6, 133.7, 133.8, 135.9, 136.0, 136.0, 139.5, 139.6, 139.9, 140.0, 140.9, 141.0, 141.4, 141.5, 143.3 (phenyl C). FT-IR (KBr, cm⁻¹): ν = 3050 (m), 2869 (w), 1952 (w), 1886 (w), 1584 (w), 1572 (w), 1538 (w), 1481 (m), 1433 (s), 1375 (m), 1309 (w), 1267 (w), 1183 (w), 1155 (w), 1129 (w), 1098 (m), 1046 (m), 1027 (w), 998 (w), 835 (m), 736 (s), 693 (s), 513 (s), 470 (m), 408 (w). Anal. Calcd. for C₆₃H₅₅N₂P₄Pd₂: C, 64.30; H, 4.71;

N, 2.38. Found: C, 64.47; H, 4.62; N, 2.24. HRMS (+ESI): Calcd m/z for $[M+2H]^{2+}$ $C_{60}H_{54}N_2P_4Pd_2$: 1138.1307, Found: 1138.1362.

Synthesis of $[Ni(OAc)_2(C_4H_8N-2,5-(CH_2PPh)_2-\kappa^3PNP)]$, 13. A solution of **2** (0.374 g, 0.805 mmol) and $[Ni(OAc)_2] \cdot 4H_2O$ (0.2 g, 0.803 mmol) in acetonitrile (30 mL) was stirred for 24 h at room temperature. The solvent was removed under vacuum to give a red colored residue which was washed with petroleum ether and dried under vacuum to give a red colored solid (0.430 g). This solid is predominantly consisting of **13** as shown by the 1H and ^{31}P NMR data. 1H NMR ($CDCl_3$, 200 MHz, ppm): δ = 1.51 (s, 3H, OAc), 3.50 (t, 4H, $^2J(P,H)$ = 4.8 Hz, CH_2), 5.90 (s, 2H, pyrrole β -CH), 7.41–7.48 (m, 12H, phenyl CH), 7.80–7.86 (m, 8H, phenyl CH). $^{31}P\{^1H\}$ NMR (161.9 MHz, $CDCl_3$, ppm): δ = 27.0(s). ^{13}C NMR ($CDCl_3$, 100.6 MHz, ppm): δ = 23.4 (s, CH_3COO), 31.8 (m, $J(C,P)$ = 13.8 Hz, CH_2), 106.2 (t, $J(C,P)$ = 5.3 Hz, pyrrole β -CH), 128.9, 129.0, 129.0, 130.6, 130.9, 131.0, 131.1, 131.3, 132.1, 132.9, 133.0, 133.0, 133.1, 133.2, 133.2, 133.4, 136.6, 136.7 (phenyl C), 177.3 (s, CH_3COO). FT-IR (KBr, cm^{-1}): ν = 3412 (m), 3052(m), 1625(s), 1483 (m), 1434 (s), 1367 (s), 1317(s), 1250 (w), 1184 (w), 1103 (m), 1066 (w), 1000 (w), 838 (w), 741 (s), 694 (s), 520 (s), 477 (m). HRMS (+ESI): Calcd m/z for $[M-OAc+2H^+K^+]^{4+}$ $C_{30}H_{28}KNNiP_2$: 561.0688, Found: 561.0298.

Synthesis of $[NiCl(C_4H_8N-2,5-(CH_2PPh)_2-\kappa^3PNP)]$, 14. Method a. A solution of **2** (0.374 g, 0.805 mmol) and $[Ni(OAc)_2] \cdot 4H_2O$ (0.2 g, 0.803 mmol) in acetonitrile (30 mL) was stirred for 24 h at room temperature. The solvent was removed under vacuum to give a red colored solid. The solid was dissolved in acetone (12 mL) to which a solution of LiCl (0.172 g, 4.01 mmol) in water (8 mL) was added. The suspension was stirred at room temperature for 48 h to give precipitate of complex **14**. The solution was filtered, and the precipitate was washed with water three times (10 mL) and dried under vacuum (0.40 g, 0.72 mmol 89% yield). Suitable single crystals were obtained from a solution of **14** in benzene upon layering with petroleum ether at room temperature.

Method b. To a mixture of $[NiCl_2(DME)]$ (0.100 g, 0.460 mmol) and **2** (0.214 g, 0.461 mmol) in acetonitrile (15 mL) was added dropwise triethylamine (0.065 mL, 0.461 mmol) with stirring at room temperature. After 24 h stirring, the solvent was removed under vacuum, and the residue was dissolved in dichloromethane. The dichloromethane solution was washed with water (3×30 mL) and dried over anhydrous Na_2SO_4 and then filtered. The solvent was removed under vacuum to give a dark brown precipitate of **14** (0.210 g, 0.377 mmol, 84% yield). 1H NMR ($CDCl_3$, 400 MHz, ppm): δ = 3.59 (t, 4H, $^2J(P,H)$ = 4.8 Hz, CH_2), 5.99 (s, 2H, pyrrole β -CH), 7.37–7.50 (m, 12H, phenyl CH), 7.86–7.91 (m, 8H, phenyl CH). $^{31}P\{^1H\}$ NMR (161.9 MHz, $CDCl_3$, ppm): δ = 30.6(s). ^{13}C NMR ($CDCl_3$, 100.6 MHz, ppm): δ = 32.0 (t, $J(C,P)$ = 13.5 Hz, CH_2), 106.1 (t, $J(C,P)$ = 5.6 Hz, pyrrole β -CH), 129.0, 129.1, 129.1, 133.0, 133.1, 133.2, 137.1 (phenyl C). FT-IR (KBr, cm^{-1}): ν = 2923(s), 2853 (m), 1586 (w), 1465 (w), 1432 (m), 1370 (w), 1303 (w), 1250 (w), 1178 (w), 1101 (m), 1066 (w), 997 (w), 833 (w), 740 (m), 690 (m), 518 (m), 479 (m). HRMS (+ESI): Calcd m/z for $[M-Cl+2H^+K^+]^{4+}$ $C_{30}H_{28}KNNiP_2$: 561.07, Found: 561.20.

Synthesis of $[NiBr(C_4H_8N-2,5-(CH_2PPh)_2-\kappa^3PNP)]$, 15. Complex **15** was synthesized using LiBr (0.349 g, 4.01 mmol) by following the above procedure (Method a) for complex **14**. To a solution of **15** in benzene (10 mL) was added slowly petroleum ether to form a layer. Brown crystals of **15** were formed after 24 h (0.390 g, 0.65 mmol, 80% yield). 1H NMR ($CDCl_3$, 400 MHz, ppm): δ = 3.62 (t, 4H, $^2J(P,H)$ = 4.8 Hz, CH_2), 6.02 (s, 2H, pyrrole β -CH), 7.37–7.50 (m, 12H, phenyl CH), 7.85–7.90 (m, 8H, phenyl CH). $^{31}P\{^1H\}$ NMR (161.9 MHz, $CDCl_3$, ppm): δ = 35.0(s). ^{13}C NMR ($CDCl_3$, 100.6 MHz, ppm): δ = 32.7 (t, $J(C,P)$ = 13.2 Hz, CH_2), 105.7 (t, $J(C,P)$ = 5.7 Hz, pyrrole β -CH), 128.7, 128.7, 128.8, 130.4, 130.6, 130.7, 133.1, 133.1, 133.2, 137.0 (phenyl C). FT-IR (KBr, cm^{-1}): ν = 3052, (m), 1661 (w), 1585 (w), 1482 (m), 1433 (s), 1369 (m), 1309 (w), 1252 (m), 1184 (w), 1101 (s), 1065 (m), 1026 (w), 998 (w) 835 (m), 739 (s), 691 (s), 518 (s), 481 (m), 445 (w). HRMS (+ESI): Calcd m/z for $[M-Br+2H^+K^+]^{4+}$ $C_{30}H_{28}KNNiP_2$: 561.07, Found: 561.16.

Synthesis of $[Ni\{C_4H_8N-2,5-(CH_2PPh)_2-\kappa^3PNP\}]$, 16. This complex was synthesized using KI (0.667 g, 4.01 mmol) by following the above procedure (Method a) for complex **14**. To a solution of **16** in benzene (10 mL) was added slowly petroleum ether to form a layer. Purple crystals of **16** were formed after 3 days (0.421 g, 0.65 mmol, 81% yield). 1H NMR ($CDCl_3$, 200 MHz, ppm): δ = 3.69 (t, 4H, $^2J(P,H)$ = 4.9 Hz, CH_2), 6.06 (s, 2H, pyrrole β -CH), 7.37–7.47 (m, 12H, phenyl CH), 7.79–7.88 (m, 8H, phenyl CH). $^{31}P\{^1H\}$ NMR (161.9 MHz, $CDCl_3$, ppm): δ = 42.6(s). ^{13}C NMR ($CDCl_3$, 50.3 MHz, ppm): δ = 34.5 (d, $J(C,P)$ = 13.1 Hz, CH_2), 105.5 (d, $J(C,P)$ = 6 Hz, pyrrole β -CH), 128.5, 128.7, 128.8, 128.9, 130.8, 131.0, 131.3, 131.7, 133.6, 133.7, 133.8, 137.3, 137.5 (phenyl C). FT-IR (KBr, cm^{-1}): ν = 3050 (m), 2924 (m), 1710 (w), 1585 (w), 1482 (m), 1433(s), 1369 (m), 1251 (m), 1185 (w), 1100 (s), 1065 (w), 998 (w), 836 (m), 739 (s), 691 (s), 517 (s), 481 (m). HRMS (+ESI): Calcd m/z for $[M-I+2H^+K^+]^{4+}$ $C_{30}H_{28}KNNiP_2$: 561.07, Found: 561.17.

X-ray Crystallography. Single crystal X-ray diffraction data collections for all the compounds were performed using Bruker-APEX-II CCD diffractometer with graphite monochromated $Mo_{K\alpha}$ radiation (λ = 0.71073 Å). The structures were solved by SIR-92⁵⁹ available in WinGX, which successfully located most of the non-hydrogen atoms. Subsequently, least-squares refinements were carried out on F^2 using SHELXL-97 (WinGX version)⁶⁰ to locate the remaining non-hydrogen atoms. All non-hydrogen atoms were refined anisotropically, and the most of the hydrogen atoms were refined isotropically on calculated positions using a riding model. In the structure of **5** and **6**, the NH and all water hydrogen atoms except the hydrogen atoms of O6 water were located and refined isotropically with restraints, SADI and their thermal parameters were set equivalent to 1.2 times the thermal parameter value of the atom to which the hydrogen atoms are bonded. The O6 water hydrogen atoms in **6** could not be located. A severely disordered one-half of the benzene molecule was found in the crystal lattice of **12**.

■ ASSOCIATED CONTENT

📄 Supporting Information

NMR, IR, HRMS spectra, crystallographic data (CIF), and packing diagrams. This material is available free of charge via the Internet at <http://pubs.acs.org>.

■ AUTHOR INFORMATION

Corresponding Author

*E-mail: gmani@chem.iitkgp.ernet.in (G.M.).

Notes

The authors declare no competing financial interest.

■ ACKNOWLEDGMENTS

We thank the DST and CSIR for support and for the X-ray and NMR facilities. We thank Dr. Carola Schulzke, Trinity College, Dublin for HRMS.

■ DEDICATION

Dedicated to Professor S. S. Krishnamurthy on the occasion of his 73rd birthday.

■ REFERENCES

- (a) Albrecht, M.; van Koten, G. *Angew. Chem., Int. Ed.* **2001**, *40*, 3750–3781. (b) van der Boom, M. E.; Milstein, D. *Chem. Rev.* **2003**, *103*, 1759–1792.
- (a) Milstein, D. *Pure Appl. Chem.* **2003**, *75*, 445–460. (b) Benito-Garagorri, D.; Kirchner, K. *Acc. Chem. Res.* **2008**, *41*, 201–213. (c) Gunanathan, C.; Milstein, D. *Acc. Chem. Res.* **2011**, *44*, 588–602. (d) Choi, J.; MacArthur, A. H. R.; Brookhart, M.; Goldman, A. S. *Chem. Rev.* **2011**, *111*, 1761–1779. (e) Niu, J.-L.; Hao, X.-Q.; Gong, J.-F.; Song, M.-P. *Dalton Trans.* **2011**, *40*, 5135–5150.
- (3) Green, M. L. H. *J. Organomet. Chem.* **1995**, *500*, 127–148.

- (4) Sattler, A.; Parkin, G. *J. Am. Chem. Soc.* **2012**, *134*, 2355–2366.
- (5) (a) Haenel, M. W.; Oevers, S.; Angermund, K.; Kaska, W. C.; Fan, H.-J.; Hall, M. B. *Angew. Chem., Int. Ed.* **2001**, *40*, 3596–3600. (b) Liu, F.; Pak, E. B.; Singh, B.; Jensen, C. M.; Goldman, A. S. *J. Am. Chem. Soc.* **1999**, *121*, 4086–4087. (c) Jensen, C. M. *Chem. Commun.* **1999**, 2443–2449. (d) Gupta, M.; Hagen, C.; Flesher, R. J.; Kaska, W. C.; Jensen, C. M. *J. Chem. Soc., Chem. Commun.* **1996**, 2083–2084.
- (6) Zhang, J.; Leitius, G.; Ben-David, Y.; Milstein, D. *J. Am. Chem. Soc.* **2005**, *127*, 10840–10841.
- (7) (a) Huang, Z.; White, P. S.; Brookhart, M. *Nature* **2010**, *465*, 598–601. (b) Ghosh, R.; Kanzelberger, M.; Emge, T. J.; Hall, G. S.; Goldman, A. S. *Organometallics* **2006**, *25*, 5668–5671.
- (8) Benito-Garagorri, D.; Kirchner, K. *Acc. Chem. Res.* **2008**, *41*, 201–213.
- (9) (a) Ohff, M.; Ohff, A.; van der Boom, M. E.; Milstein, D. *J. Am. Chem. Soc.* **1997**, *119*, 11687–11688. (b) Morales-Morales, D.; Redón, R.; Yung, C.; Jensen, C. M. *Chem. Commun.* **2000**, 1619–1620. (c) Miyazaki, F.; Yamaguchi, K.; Shibasaki, M. *Tetrahedron Lett.* **1999**, *40*, 7379–7383.
- (10) Ren, P.; Vechorkin, O.; von Allmen, K.; Scopelliti, R.; Hu, X. *J. Am. Chem. Soc.* **2011**, *133*, 7084–7095.
- (11) (a) Johnson, L. K.; Killian, C. M.; Brookhart, M. *J. Am. Chem. Soc.* **1995**, *117*, 6414–6415. (b) Ittel, S. D.; Johnson, L. K.; Brookhart, M. *Chem. Rev.* **2000**, *100*, 1169–1203.
- (12) Selander, N.; Szabó, K. *J. Chem. Rev.* **2011**, *111*, 2048–2076.
- (13) (a) Rytchinski, B.; Oevers, S.; Montag, M.; Vignalok, A.; Rozenberg, H.; Martin, J. M. L.; Milstein, D. *J. Am. Chem. Soc.* **2001**, *123*, 9064–9077. (b) van der Boom, M. E.; Kraatz, H.-B.; Hassner, L.; Ben-David, Y.; Milstein, D. *Organometallics* **1999**, *18*, 3873–3884.
- (14) Gandelman, M.; Milstein, D. *Chem. Commun.* **2000**, 1603–1604.
- (15) van der Boom, M. E.; Liou, S.-Y.; Ben-David, Y.; Shimon, L. J. W.; Milstein, D. *J. Am. Chem. Soc.* **1998**, *120*, 6531–6541.
- (16) Liang, L.-C.; Chien, P.-S.; Huang, Y.-L. *J. Am. Chem. Soc.* **2006**, *128*, 15562–15563.
- (17) (a) Lee, D. W.; Jensen, C. M.; Morales-Morales, D. *Organometallics* **2003**, *22*, 4744–4749. (b) Renkema, K. B.; Kissin, Y. V.; Goldman, A. S. *J. Am. Chem. Soc.* **2003**, *125*, 7770–7771. (c) Göttker-Schnetmann, I.; White, P. S.; Brookhart, M. *Organometallics* **2004**, *23*, 1766–1776. (d) Lee, H. M.; Zeng, J. Y.; Hu, C.-H.; Lee, M.-T. *Inorg. Chem.* **2004**, *43*, 6822–6829. (e) Ma, L.; Woloszynek, R. A.; Chen, W.; Ren, T.; Protasiewicz, J. D. *Organometallics* **2006**, *25*, 3301–3304. (f) Olsson, D.; Wendt, O. F. *J. Organomet. Chem.* **2009**, *694*, 3112–3115. (g) Punji, B.; Emge, T. J.; Goldman, A. S. *Organometallics* **2010**, *29*, 2702–2709. (h) Salah, A. B.; Offenstein, C.; Zargarian, D. *Organometallics* **2011**, *30*, 5352–5364. (i) Bhattacharya, P.; Krause, J. A.; Guan, H. *Organometallics* **2011**, *30*, 4720–4729. (j) Adams, J. J.; Lau, A.; Arulsamy, N.; Roddick, D. M. *Organometallics* **2011**, *30*, 689–696. (k) Adams, J. J.; Arulsamy, N.; Roddick, D. M. *Organometallics* **2011**, *30*, 697–711. (l) Schuster, E. M.; Botoshansky, M.; Gandelman, M. *Angew. Chem., Int. Ed.* **2008**, *47*, 4555–4558.
- (18) (a) Poverenov, E.; Gandelman, M.; Shimon, L. J. W.; Rozenberg, H.; Ben-David, Y.; Milstein, D. *Organometallics* **2005**, *24*, 1082–1090. (b) Yang, M.-J.; Liu, Y.-J.; Gong, J.-F.; Song, M.-P. *Organometallics* **2011**, *30*, 3793–3803. (c) Spasyuk, D. M.; Gorelsky, S. I.; van der Est, A.; Zargarian, D. *Inorg. Chem.* **2011**, *50*, 2661–2674. (d) Herbert, D. E.; Ozerov, O. V. *Organometallics* **2011**, *30*, 6641–6654.
- (19) (a) Zeng, G.; Li, S. *Inorg. Chem.* **2011**, *50*, 10572–10580. (b) Lindner, R.; van den Bosch, B.; Lutz, M.; Reek, J. N. H.; van der Vlugt, J. I. *Organometallics* **2011**, *30*, 499–510.
- (20) (a) Fryzuk, M. D. *Can. J. Chem.* **1992**, *70*, 2839–2845. (b) Jia, G.; Lee, H. M.; Williams, I. D. *Organometallics* **1997**, *16*, 3941–3949. (c) Ozerov, O. V.; Guo, C.; Fan, L.; Foxman, B. M. *Organometallics* **2004**, *23*, 5573–5580. (d) Cochran, B. M.; Michael, F. E. *J. Am. Chem. Soc.* **2008**, *130*, 2786–2792. (e) van der Vlugt, J. I.; Reek, J. N. H. *Angew. Chem., Int. Ed.* **2009**, *48*, 8832–8846. (f) van der Vlugt, J. I.; Lutz, M.; Pidko, E. A.; Vogt, D.; Spek, A. L. *Dalton Trans.* **2009**, 1016–1023. (g) Gunanathan, C.; Gnanaprakasam, B.; Iron, M. A.; Shimon, L. J. W.; Milstein, D. *J. Am. Chem. Soc.* **2010**, *132*, 14763–14765. (h) Langer, R.; Diskin-Posner, Y.; Leitius, G.; Shimon, L. J. W.; Ben-David, Y.; Milstein, D. *Angew. Chem., Int. Ed.* **2011**, *50*, 9948–9952. (i) Kundu, S.; Brennessel, W. W.; Jones, W. D. *Inorg. Chem.* **2011**, *50*, 9443–9453. (j) Chaplin, A. B.; Weller, A. S. *Organometallics* **2011**, *30*, 4466–4469. (k) Johnson, K. R. D.; Hayes, P. G. *Organometallics* **2011**, *30*, 58–67.
- (21) Moulton, C. J.; Shaw, B. L. *J. Chem. Soc., Dalton Trans.* **1976**, 1020–1024.
- (22) (a) Mazet, C.; Gade, L. H. *Organometallics* **2001**, *20*, 4144–4146. (b) Mazet, C.; Gade, L. H. *Chem.—Eur. J.* **2002**, *8*, 4308–4318. (c) Mazet, C.; Gade, L. H. *Chem.—Eur. J.* **2003**, *9*, 1759–1767. (d) Mazet, C.; Gade, L. H. *Eur. J. Inorg. Chem.* **2003**, 1161–1168. (e) Mazet, C.; Gade, L. H. *Inorg. Chem.* **2003**, *42*, 210–215. (f) Okamoto, K.; Kanbara, T.; Yamamoto, T. *Chem. Lett.* **2006**, *35*, 558–559. (g) Bröring, M.; Kleeberg, C. *Inorg. Chim. Acta* **2007**, *360*, 3281–3286. (h) Capacchione, C.; Wadepohl, H.; Gade, L. H. *Z. Anorg. Allg. Chem.* **2007**, *633*, 2131–2134. (i) Konrad, F.; Fillo, J. L.; Rettenmeier, C.; Wadepohl, H.; Gade, L. H. *Eur. J. Inorg. Chem.* **2009**, 4950–4961. (j) Konrad, F.; Lloret Fillo, J.; Wadepohl, H.; Gade, L. H. *Inorg. Chem.* **2009**, *48*, 8523–8535. (k) Wanniarachchi, S.; Liddle, B. J.; Lindeman, S. V.; Gardinier, J. R. *J. Organomet. Chem.* **2011**, *696*, 3623–3636. (l) Li, R.; Brooker, S. *Inorg. Chim. Acta* **2011**, *365*, 246–250. (m) Wang, L.; Liu, D.; Cui, D. *Organometallics* **2012**, *31*, 6014–6021.
- (23) Ghorai, D.; Kumar, S.; Mani, G. *Dalton Trans.* **2012**, *41*, 9503–9512.
- (24) Grüger, N.; Wadepohl, H.; Gade, L. H. *Dalton Trans.* **2012**, DOI: 10.1039/C2DT32199H.
- (25) Davies, J. A.; Dutremez, S.; Pinkerton, A. A. *Inorg. Chem.* **1991**, *30*, 2380–2387.
- (26) (a) Silva, M. R.; Beja, A. M.; Paixão, J. A.; Sobral, A. J. F. N.; Lopes, S. H.; Gonsalves, A. M. d. A. *Acta Crystallogr., Sect. C* **2002**, *C58*, o572–o574. (b) Malone, J. F.; Murray, C. M.; Charlton, M. H.; Docherty, R.; Lavery, A. J. *J. Chem. Soc., Faraday Trans.* **1997**, *93*, 3429–3436.
- (27) (a) Rapko, B. M.; Duesler, E. N.; Frutos, D.; Paine, R. T. *Polyhedron* **1995**, *14*, 2361–2369. (b) Tan, Y.-C.; Gan, X.-M.; Stanchfield, J. L.; Duesler, E. N.; Paine, R. T. *Inorg. Chem.* **2001**, *40*, 2910–2913.
- (28) (a) Trzeciak, A. M.; Ciunik, Z.; Ziolkowski, J. J. *Organometallics* **2002**, *21*, 132–137. (b) Nuricumbo-Escobar, J. J.; Campos-Alvarado, C.; Rios-Moreno, G.; Morales-Morales, D.; Walsh, P. J.; Parra-Hake, M. *Inorg. Chem.* **2007**, *46*, 6182–6189.
- (29) Fryzuk, M. D.; MacNeil, P. A.; Rettig, S. J.; Secco, A. S.; Trotter, J. *Organometallics* **1982**, *1*, 918–930.
- (30) Feller, M.; Ari-Ben, E.; Iron, M. A.; Posner-Diskin, Y.; Leitius, G.; Shimon, L. J. W.; Konstantinovski, L.; Milstein, D. *Inorg. Chem.* **2010**, *49*, 1615–1625.
- (31) Lansing, B. R., Jr.; Goldberg, K. I.; Kemp, R. A. *Dalton Trans.* **2011**, *40*, 8950–8958.
- (32) Benito-Garagorri, D.; Bocokić, V.; Mereiter, K.; Kirchner, K. *Organometallics* **2006**, *25*, 3817–3823.
- (33) Kimmich, B. F. M.; Marshall, W. J.; Fagan, P. J.; Hauptman, E.; Bullock, R. M. *Inorg. Chim. Acta* **2002**, *330*, 52–58.
- (34) This complex is probably formed via oxidative addition reactions of the ligand with the Pd(0) complex, giving initially a complex containing two Pd-H groups which is expected to eliminate H₂. However, the signal for H₂ could not be detected from the reaction between 20 mg of [Pd₂(dba)₃]₂·CHCl₃ and 20 mg of **2** in toluene-*d*₆ in a NMR tube. Hence, after oxidative addition of the pincer ligand, it is possible that the in situ formed ‘Pd-H’ species could have become involved in reduction reactions with dibenzylideneacetone (dba) by which metal hydrides are consumed to form the final product **12**. As a support, the HRMS (+ESI) spectrum of this reaction mixture showed a peak *m/z* at 237.1207 (Calcd *m/z* for [M+H]⁺ C₁₇H₁₇O: 237.1279) which corresponds to either PhCH=CHC(O)(CH₂)₂Ph or PhCH=CHCH(OH)CH=CHPh, the reduced product of dba.

- (35) Zhang, J.; Pattacini, R.; Braunstein, P. *Inorg. Chem.* **2009**, *48*, 11954–11962.
- (36) (a) Wachtler, H.; Schuh, W.; Ongania, K.-H.; Kopacka, H.; Wurst, K.; Peringer, P. *J. Chem. Soc., Dalton Trans.* **2002**, 2532–2535. (b) Song, H.-B.; Zhang, Z.-Z.; Mak, T. C. W. *Inorg. Chem. Commun.* **2002**, *5*, 442–445.
- (37) (a) Tani, K.; Nakamura, S.; Yamagata, T.; Kataoka, Y. *Inorg. Chem.* **1993**, *32*, 5398–5401. (b) Deeken, S.; Motz, G.; Bezugly, V.; Borrmann, H.; Wagner, F. R.; Kempe, R. *Inorg. Chem.* **2006**, *45*, 9160–9162. (c) Smith, D. A.; Batsanov, A. S.; Costuas, K.; Edge, R.; Apperley, D. C.; Collison, D.; Halet, J.-F.; Howard, J. A. K.; Dyer, P. W. *Angew. Chem., Int. Ed.* **2010**, *49*, 7040–7044.
- (38) Fafard, C. M.; Adhikari, D.; Foxman, B. M.; Mindiola, D. J.; Ozerov, O. V. *J. Am. Chem. Soc.* **2007**, *129*, 10318–10319.
- (39) Baya, M.; Houghton, J.; Konya, D.; Champouret, Y.; Daran, J.-C.; Almeida Leñro, K. Q.; Schoon, L.; Mul, W. P.; van Oort, A. B.; Meijboom, N.; Drent, E.; Orpen, A. G.; Poli, R. *J. Am. Chem. Soc.* **2008**, *130*, 10612–10624.
- (40) Bondi, A. J. *Phys. Chem.* **1964**, *68*, 441–451.
- (41) Spasyuk, D. M.; Zargarian, D.; van der Est, A. *Organometallics* **2009**, *28*, 6531–6540.
- (42) Liang, L.-C.; Chien, P.-S.; Lin, J.-M.; Huang, M.-H.; Huang, Y.-Y.; Liao, J.-H. *Organometallics* **2006**, *25*, 1399–1411.
- (43) van der Boom, M. E.; Liou, S.-Y.; Shimon, L. J. W.; Ben-David, Y.; Milstein, D. *Inorg. Chim. Acta* **2004**, *357*, 4015–4023.
- (44) Bachman, G. B.; Heisey, L. B. *J. Am. Chem. Soc.* **1946**, *68*, 2496–2499.
- (45) Mani, G.; Guchhait, T.; Kumar, R.; Kumar, S. *Org. Lett.* **2010**, *12*, 3910–3913.
- (46) Ukai, T.; Kawazura, H.; Ishii, Y.; Bonnet, J. J.; Ibers, J. A. *J. Organomet. Chem.* **1974**, *65*, 253–266.
- (47) Drew, D.; Doyle, J. R.; Shaver, A. G. *Inorg. Synth.* **1990**, *28*, 346–349.
- (48) Anderson, G. K.; Lin, M.; Sen, A.; Gretz, E. *Inorg. Synth.* **1990**, *28*, 60–63.
- (49) Ward, L. G. L.; Pipal, J. R. *Inorg. Synth.* **1971**, *13*, 154–164.
- (50) Wittenberg, D.; Gilman, H. *J. Org. Chem.* **1958**, *23*, 1063–1065.
- (51) Frisch, M. J.; Trucks, G. W.; Schlegel, H. B.; Scuseria, G. E.; Robb, M. A.; Cheeseman, J. R.; Scalmani, G.; Barone, V.; Mennucci, B.; Petersson, G. A.; Nakatsuji, H.; Caricato, M.; Li, X.; Hratchian, H. P.; Izmaylov, A. F.; Bloino, J.; Zheng, G.; Sonnenberg, J. L.; Hada, M.; Ehara, M.; Toyota, K.; Fukuda, R.; Hasegawa, J.; Ishida, M.; Nakajima, T.; Honda, Y.; Kitao, O.; Nakai, H.; Vreven, T.; Montgomery Jr, J. A.; Peralta, J. E.; Ogliaro, F.; Bearpark, M.; Heyd, J. J.; Brothers, E.; Kudin, K. N.; Staroverov, V. N.; Kobayashi, R.; Normand, J.; Raghavachari, K.; Rendell, A.; Burant, J. C.; Iyengar, S. S.; Tomasi, J.; Cossi, M.; Rega, N.; Millam, N. J.; Klene, M.; Knox, J. E.; Cross, J. B.; Bakken, V.; Adamo, C.; Jaramillo, J.; Gomperts, R.; Stratmann, R. E.; Yazyev, O.; Austin, A. J.; Cammi, R.; Pomelli, C.; Ochterski, J. W.; Martin, R. L.; Morokuma, K.; Zakrzewski, V. G.; Voth, G. A.; Salvador, P.; Dannenberg, J. J.; Dapprich, S.; Daniels, A. D.; Farkas, Ö.; Foresman, J. B.; Ortiz, J. V.; Cioslowski, J.; Fox, D. J. *Gaussian 09*, Revision A.1; Gaussian Inc.: Wallingford, CT, 2009.
- (52) Dennington, R.; Keith, T.; Millam, J. *GaussView*, Version 3.0; Semichem Inc.: Shawnee Mission, KS, 2009.
- (53) *Amsterdam Density Functional (ADF) program*, Version 2012.01; Vrije Universiteit: Amsterdam, Netherlands, 1997.
- (54) Vega, A.; Jean-Yves, S. *Inorg. Chem.* **2004**, *43*, 4012–4018.
- (55) (a) Becke, A. D. *J. Chem. Phys.* **1986**, *84*, 4524–4529. (b) Becke, A. D. *Phys. Rev. A: At., Mol., Opt. Phys.* **1988**, *38*, 3098–3100.
- (56) (a) Perdew, J. P. *Phys. Rev. B: Condens. Matter Mater. Phys.* **1986**, *33*, 8822–8824. (b) Perdew, J. P. *Phys. Rev. B: Condens. Matter Mater. Phys.* **1986**, *34*, 7406–7406.
- (57) (a) van Lenthe, E.; Baerends, E. J.; Snijders, J. G. *J. Chem. Phys.* **1993**, *99*, 4597–4601. (b) van Lenthe, E.; Baerends, E. J.; Snijders, J. G. *J. Chem. Phys.* **1994**, *101*, 9783–9792. (c) van Lenthe, E.; van Leeuwen, R.; Baerends, E. J. *Int. J. Quantum Chem.* **1996**, *57*, 281–293.
- (58) Ziegler, T. In *Metal Ligand Interactions: From Atoms to Clusters to Surfaces*; Salahub, D. R., Russo, N., Eds.; Kluwer: Dordrecht, The Netherlands, 1992; p 367.
- (59) Altomare, A.; Cascarano, G.; Giacovazzo, C.; Guagliardi, A. J. *Appl. Crystallogr.* **1993**, *26*, 343–350.
- (60) Sheldrick, G. M. *Acta Crystallogr.* **2008**, *A64*, 112–122.